Energy Research and Development Division

FINAL PROJECT REPORT

Solar-Reflective "Cool" Walls: Benefits, Technologies, and Implementation

Appendix I: Metrics and Methods to Assess Cool Wall Performance (Task 4.1 Report)

California Energy Commission
Gavin Newsom, Governor

April 2019 | CEC-500-2019-040-API

Appendix I:
Metrics and methods to assess cool wall performance (Task 4.1 report)

Ronnen Levinson[1], Hugo Destaillats[1], Sharon Chen[1], Paul Berdahl[1], and Haley Gilbert[1]

[1] Heat Island Group, Lawrence Berkeley National Laboratory

28 February 2018

1 Introduction

The ability of a wall product to stay cool in the sun depends on its solar reflectance and thermal emittance. High solar reflectance reduces solar heat gain (absorption of sunlight), while high thermal emittance helps cool the surface through long-wave radiative exchange with its environment. Wall product performance is further described by additional surface properties including solar spectral reflectance, color, soil resistance, and hydrophilicity/hydrophobicity. This report addresses the metrics and methods needed to assess the evolution of the surface properties of a wall product over its service life.

2 Properties

Here we describe each property of interest.

2.1 Solar spectral reflectance

Solar spectral reflectance (symbol r) is the variation of reflectance (fraction of incident light reflected) with wavelength over the solar spectrum. Reflectance at each wavelength ranges from 0 to 1 (or 0 to 100 percent), and can vary with the geometry of incident sunlight. Solar spectral reflectance can be used to calculate solar (0.3 to 2.5 μm), ultraviolet (0.3 – 0.4 μm), visible (0.4 – 0.7 μm), and near-infrared (NIR, 0.7 – 2.5 μm) broadband reflectances, as well as color. Colorants (pigments and dyes) and soiling agents (soot, dust, organic matter) can be identified from their spectral reflectance signatures. Solar spectral reflectance can also be used to identify "cool colored" surfaces whose solar reflectances are boosted by high NIR reflectance.

2.2 Solar reflectance

Solar reflectance (abbreviation SR; symbol ρ) is the fraction of incident sunlight reflected by a surface. The solar reflectance of a given surface can vary with the spectrum (distribution of power by wavelength) and geometry (angular distribution) of incident sunlight. Solar reflectance ranges from 0 to 1 (or 0 to 100 percent).

2.3 Color

Color is an important aesthetic property of many building envelope surfaces. Color is often identified by coordinates in a color space, such as CIELAB or HunterLAB.

2.4 Effective solar reflectance

If a surface re-emits at longer wavelengths light absorbed at shorter wavelengths, or fluoresces, it will exhibit an effective solar reflectance (abbreviation ESR; symbol ρ_{eff}) that is the fraction of incident solar power rejected by the combination of reflection and fluorescence. Like solar reflectance, effective solar reflectance ranges from 0 to 1 (or 0 to 100 percent).

2.5 Solar retroreflectance

A retroreflective surface reflects incident light to its origin. Solar retroreflectance is the fraction of incident sunlight reflected toward the sun. High solar retroreflectance could reduce both wall solar heat gain and the fraction of *wall-reflected* sunlight incident on other surfaces in the city. That is, while about 50% of global sunlight diffusely reflected from a wall, and all beam sunlight specularly reflected from a wall, will strike neighboring wall or ground surfaces, beam sunlight ideally retroreflected from a wall will return entirely to the solar disc. Ideal solar retroreflection can also minimize glare, since any path that permits the incidence of beam sunlight must be free of observers.

We address properties needed to assess solar retroreflectance in our Task 5.3 report: *Development of retroreflective materials.*

2.6 Thermal emittance

Thermal emittance (abbreviation TE; symbol ε) is the ratio of radiant energy emitted by a surface near 300 K (about 27˚C, or 80˚F) to that emitted by a black body (perfect absorber and emitter) at the same temperature. The thermal emittance of a given surface can vary with the angle at which the emitted radiation is observed. Thermal emittance ranges from 0 to 1 (or 0 to 100%).

2.7 Initial radiative properties

Initial radiative properties are those measured before exposure.

2.8 Field-exposed aged radiative properties

Natural exposure can change the radiative properties of an exterior building envelope surface over time. “Field-exposed” aged radiative properties are measured after several years of natural exposure, following a protocol that specifies the location, geometry, and duration of the exposure.

2.9 Soiling resistance

Radiative properties of building envelope surfaces change over time due to weathering and soiling. We define as weathering all physical and chemical processes associated with material degradation due to exposure to the natural environment, driven by sunlight, thermal and humidity cycles. Soiling comprises the atmospheric deposition of debris, particulates and chemical species, as well as the growth of microbia (e.g., bacteria, fungi). Collectively, weathering and soiling contribute to material aging. In highly reflective materials, losses of performance can amount to as much as 20-30% of the initial solar reflectance (Sleiman et al. 2011). These losses can be translated to significant reductions in the energy savings achieved for a given reference building stock. For this reason, roofing materials are rated using their radiative properties measured after three years of natural exposure. A similar loss of performance can be expected for many wall products. Several technologies are currently available to prevent or reduce the amount of soiling depositing on the surface of materials. Such “soil-resistant” products are likely to contribute major building energy savings.

Absolute and/or fractional changes in radiative properties (e.g., loss of solar reflectance) upon natural exposure may be evaluated to gauge the ability of a “cool” product to stay clean and maintain its high solar reflectance. “Relative” soiling resistance can be evaluated by comparing reflectance loss to that experienced by a reference product of the same initial solar reflectance. “Absolute” soiling resistance can be assessed by comparing reflectance loss to that which would be experienced if the surface were fully covered with an opaque soil layer.

2.10 Hydrophilicity/hydrophobicity

The ability of a solid surface to attract or repel water can affect its resistance to soiling. Superhydrophobic coatings with dramatically increased water contact angles can be achieved by microtexturing features that produce the “Lotus effect” and minimize the contact of surfaces with water and soiling agents. Such limited contact facilitates subsequent mechanical removal of particles and evaporation (Schaeffer et al. 2015). Superhydrophilic coatings applied primarily to self-cleaning window glass typically comprise a thin layer of a photocatalyst (anatase TiO_2). In the presence of sunlight, the TiO_2 increases the wettability of the surface, and helps form continuous water films that facilitate runoff of soiling deposits. The photocatalytic process can also remove some of the soiling agents deposited on the surface by chemical oxidation to volatile species (Chabas et al. 2014).

3 Metrics

Here we specify the metric by which each surface property is to be evaluated.

3.1 Solar spectral reflectance

We will assess near normal-hemispherical spectral reflectance over the wavelength range 250 – 2,500 nm (0.25 – 2.5 μm) at an interval of 5 nm. This reflectance is readily measurable with a UV-VIS-NIR (a.k.a. solar) benchtop spectrometer equipped with an integrating sphere. Past experience with roofing products suggests that a wavelength interval of 5 nm should provide sufficient spectral detail.

Since the spectrum 250 – 300 nm contains almost no solar energy, it is acceptable to measure solar spectral reflectance over the more limited wavelength range 300 – 2,500 nm. However, reflectance in the 250 – 300 nm portion of the UV spectrum can occasionally provide insight into material properties, and is within the measurement range of a typical solar UV-VIS-NIR spectrometer.

3.2 Solar reflectance

We will assess air mass 1.5 (AM1.5) global-hemispherical solar reflectance under the solar conditions for a sun-facing vertical surface specified by ASTM G197-14 (Standard Table for Reference Solar Spectral Distributions: Direct and Diffuse on 20° Tilted and Vertical Surfaces) (ASTM 2014). Task Report Appendix A details the process by which this particular metric, hereafter called AM1.5 global vertical (AM1.5GV) solar reflectance, was selected.

3.3 Color

We will calculate CIELAB color coordinates (L*, a*, b*) from 360 – 780 nm spectral reflectance following ASTM E308-15 (Standard Practice for Computing the Colors of Objects by Using the CIE System) (ASTM 2015c). We will select the D65 daylight illuminant and 10° observer.

3.4 Effective solar reflectance

The effective solar absorptance (abbreviation ESA; symbol α_{eff}) of a fluorescent surface is the fraction of incident solar energy that is neither reflected nor fluoresced. We will assess the ESR of an opaque fluorescent surface by subtracting its ESA from unity. We will determine the ESA of a test surface by comparing its temperature in the sun to those of non-fluorescent, opaque reference surfaces of known solar absorptance α (1 – solar reflectance ρ). That is, if T, T_1, and T_2 are the temperatures of the test surface, first reference surface, and second reference surface, respectively, and α_1 and α_2 are the solar absorptances of the two reference surfaces, then the ESA of the test surface is

$$\alpha_{eff} = \alpha_1 + (\alpha_2 - \alpha_1)\,(T - T_1) / (T_2 - T_1) \quad (1)$$

and the ESR of the test surface is

$$\rho_{eff} = 1 - \alpha_{eff}. \quad (2)$$

3.5 Solar retroreflectance

We address metrics needed to assess solar retroreflectance in our Task 5.3 report: *Development of retroreflective materials.*

3.6 Thermal emittance

We will assess hemispherical thermal emittance, the thermal emittance metric used for roofing products.

3.7 Initial radiative properties

We will assess initial radiative properties (solar spectral reflectance, solar reflectance, thermal emittance) before exposure.

3.8 Field-exposed aged radiative properties

Starting at month three, we will assess radiative properties every three months over the course of two years of field exposure. Since exposure is slated to begin in March 2016 and end in March 2018, we will include the results for the first six or seven quarters of exposure in the Cool Walls Natural Exposure task report due in December 2017, and add the results for the remaining quarter(s) to the Cool Walls Final Report due in April 2018.

3.9 Solar reflectance loss

Exposure tends to reduce the solar reflectance of a “cool” wall product. Therefore, to try to keep changes in SR positive, we will assess solar reflectance *loss*, defined as initial solar reflectance minus aged solar reflectance. Note that the solar reflectance of some products can increase over time through processes including fading, chalking, or deposition of higher-reflectance soiling matter. In that case, the solar reflectance loss would be negative.

3.10 Thermal emittance gain

Exposure tends to increase the thermal emittance of a metallic surface, and have little to no effect on that of a non-metallic surface. Therefore, to try to keep changes in TE positive, we will assess thermal emittance *gain*, defined as aged thermal emittance minus initial thermal emittance. If thermal emittance decreases, the thermal emittance gain will be negative.

3.11 Soiling resistance

By soiling resistance, we define the ability of a particular surface to retain its initial radiative performance by either avoiding the buildup of soiling, facilitating the removal of soiling, or both. Under "soiling" we include atmospheric deposition (inert inorganic species and organic materials), reactive inorganic species and their reaction byproducts, and microbial growth. The methodology does not allow for a separate analysis of each of these factors, which are usually present simultaneously.

We will assess soiling resistance with two metrics. The first metric, "relative soiling resistance" (symbol β_{rel}), compares loss of solar reflectance to that experienced by a reference material of equal initial solar reflectance ρ_i. If the test surface and the reference surface have aged solar reflectances ρ_a and $\rho_{a,ref}$, respectively, then

$$\beta_{rel} = 1 - (\rho_i - \rho_a) / (\rho_i - \rho_{a,ref}) \quad (3)$$

If β_{rel} is zero, the surface lost exactly as much solar reflectance as the reference surface. If β_{rel} is unity, the surface lost no solar reflectance. The metric β_{rel} can be less than zero (surface lost more solar reflectance than did the reference surface) or greater than one (solar reflectance increased).

The second metric, "absolute soiling resistance" (symbol β_{abs}), compares loss of solar reflectance to that which would result from covering the surface with an opaque soil layer of solar reflectance $\rho_{soil.}$ If the test surface has initial solar reflectance ρ_i and aged solar reflectance ρ_a, respectively, then

$$\beta_{abs} = (\rho_a - \rho_{soil}) / (\rho_i - \rho_{soil}) \quad (4)$$

If β_{abs} is zero, the surface is fully soiled ($\rho_a = \rho_{soil}$); if β_{abs} is unity, the surface is unsoiled. Note that β_{abs} can not be evaluated if $\rho_i = \rho_{soil}$. We will assume $\rho_{soil} = 0.2$ based on our prior analysis of the soiling of roofing materials (Sleiman et al. 2011).

3.12 Hydrophilicity/hydrophobicity

We will assess water contact angle (abbreviation WCA; symbol θ_c), or angle at which the water-air interface meets the surface. A surface with $\theta_c < 90^\circ$ is called hydrophilic (water attracting), while one with $\theta_c > 90^\circ$ is called hydrophobic (water repelling). Water contact angle can range from 0° (water drop goes flat) for a perfectly hydrophilic surface to over 150° (water drop nearly spherical) for a superhydrophobic surface.

3.13 Solar reflectance index

Solar reflectance index (abbreviation SRI; no symbol) is a calculated "coolness" metric that relates the steady-state temperature of a well-insulated test surface in the sun to those of reference white and black surfaces. A surface that attains the same temperature as the

reference black is assigned an SRI of 0, while a surface that attains the same temperature as the reference white is assigned an SRI of 100. (Note that SRI is neither a fraction nor a percentage.) SRI typically ranges from 0 to 100, but can be lower than 0 if the surface is warmer than the reference black, or higher than 100 if the surface is cooler than the reference white.

SRI is computed from measured values of solar reflectance and thermal emittance under assumed environmental conditions. ASTM E1980-11 (Standard Practice for Calculating Solar Reflectance Index of Horizontal and Low-Sloped Opaque Surfaces) (ASTM 2011) specifies a set of environmental conditions, including solar irradiance and long-wave radiative exchange temperature, consistent with horizontal surface on a sunny summer afternoon. These environmental conditions would have to be revised to compute the SRI of a vertical surface, such as a wall. For example, incident sunlight could be based on the ASTM G197 AM1.5 global solar irradiance a sun-facing, vertical surface (about 800 W/m²), while the wall could be assumed to exchange half of its long-wave radiative exchange with the sky, and half with the ground and other walls. Wall SRI will not be calculated at this time, but could be computed if and when ASTM E1980 is extended to vertical surfaces.

4 Methods

Here we specify the method(s) by which each surface metric is to be evaluated.

4.1 Solar spectral reflectance

We will measure near normal-hemispherical solar spectral reflectance r(λ) following ASTM E903-12 (Standard Test Method for Solar Absorptance, Reflectance, and Transmittance of Materials Using Integrating Sphere) (ASTM 2012). We will use a Perkin-Elmer Lambda 900 UV-VIS-NIR benchtop spectrometer equipped with 150 mm Labsphere integrating sphere (Figure 1a-c). Three non-overlapping measurement spots will be chosen along a diagonal spanning the face of each specimen, and their results averaged.

When measuring soiled specimens, it is important to avoid contaminating the integrating sphere. An ideal but expensive and uncommon solution is to acquire a sphere with a bottom-mounted horizontal sample port. If the integrating sphere has a side-mounted vertical sample port, a quartz window should be installed over the port to prevent contamination (Figure 1d-f).

The following protocol will be used to correct spectral reflectance measurements for the effect of the window. Note that steps 1 and 2 are performed without the window installed in front of the sample port, while steps 4 through 6 are performed with the window installed in front of the spectrometer sample port.

1. Calibrate spectrometer with white calibration standard (Labsphere Spectralon SRS-99).

2. Measure spectral reflectances of void (a.k.a., light trap) [low reflectance, $r_L(\lambda)$] and white calibration standard [high reflectance, $r_H(\lambda)$].

3. Clean the window and window accessories appropriately (e.g. with glass cleaner, compressed air). Ensure these items are free of fingerprints, dust, and other contaminants.

4. Install window in front of the spectrometer sample port. <u>Do not recalibrate the spectrometer after installation.</u>

5. Re-measure spectral reflectances of void [$r_L'(\lambda)$] and white calibration standard [$r_H'(\lambda)$].

6. Measure spectral reflectance of one or more soiled specimens [$r_S'(\lambda)$].

7. Correct the spectral reflectance [$r_S'(\lambda)$] of each soiled specimen measured through the window as follows to obtain

$$r_S(\lambda) = r_L(\lambda) + [r_H(\lambda) - r_L(\lambda)] \times [r_S'(\lambda) - r_L'(\lambda)] / [r_H'(\lambda) - r_L'(\lambda)] \quad (5)$$

where

$r_S(\lambda)$ = spectral reflectance of specimen, measured through window, corrected;

$r_L(\lambda)$ = spectral reflectance of void;

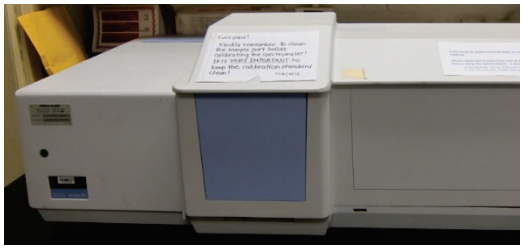

(a)

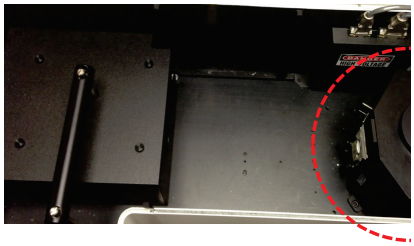

(b)

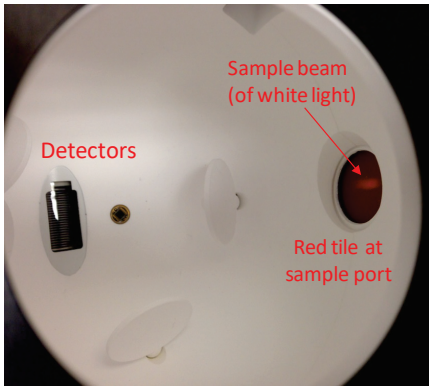

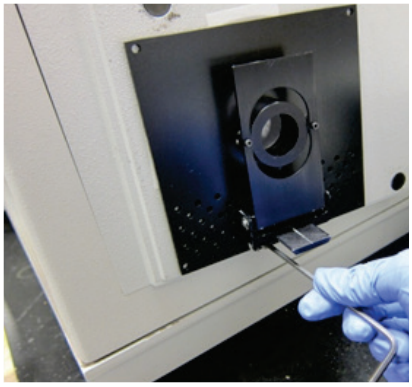

(d)

(c)

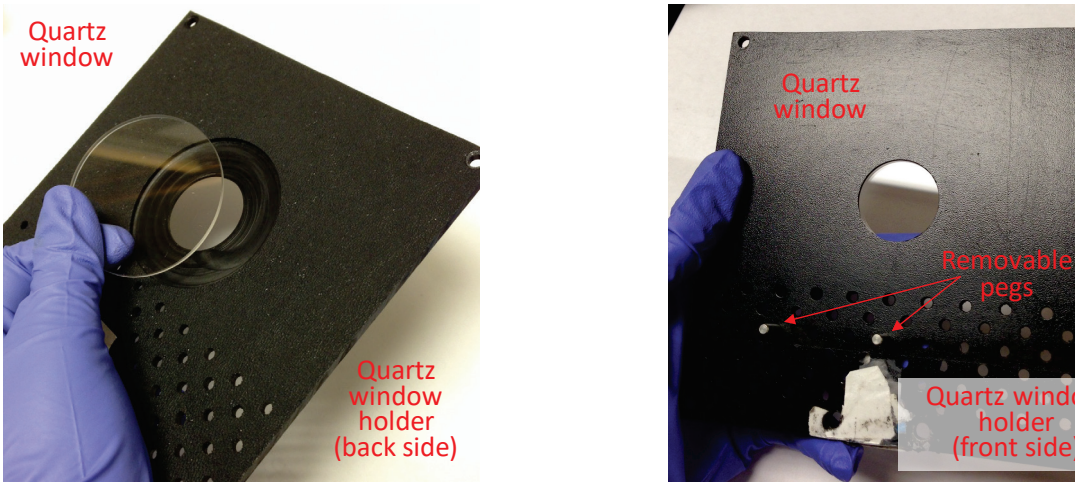

(e) (f)

Figure 1. Images of the PerkinElmer Lambda 900 UV-VIS-NIR spectrometer and its accessories, including (a) front view of closed spectrometer; (b) top view of open spectrometer, with integrating sphere accessory circled; (c) top view of open sphere; (d) side-mounted reflectance sample port fitted with quartz window; (e) window and window holder, as seen from sphere; and (f) window holder as seen from specimen.

$r_H(\lambda)$ = spectral reflectance of white calibration standard;

$r_S'(\lambda)$ = spectral reflectance of specimen, measured through window, uncorrected;

$r_L'(\lambda)$ = spectral reflectance of void, measured through window, uncorrected; and

$r_H'(\lambda)$ = spectral reflectance of white calibration standard, measured through window, uncorrected.

The uncorrected, corrected, and true solar spectral reflectances of a variety of roofing products are shown in Figure 2.

4.2 Solar reflectance

Instruments commonly used to measure solar reflectance include a UV-VIS-NIR spectrometer, a solar reflectometer, and a pyranometer (Levinson et al. 2010b).

4.2.1 Spectrometer

Following ASTM E903, we will measure near normal-hemispherical solar spectral reflectance with a UV-VIS-NIR spectrometer, then calculate AM1.5GV solar reflectance by averaging the spectral reflectance weighted by AM1.5GV solar spectral irradiance.

This “laboratory” version of AM1.5GV solar reflectance uses entirely near normal irradiance (incidence angle ~ 10°), while the “reference” AM1.5GV solar reflectance assumes that 82% of irradiance is beam light, incident at 42° from surface normal, and the remaining 18% is diffuse light. Laboratory AM1.5GV SR exactly matches reference AM1.5GV SR if the surface is perfectly matte (reflectance independent of incidence angle). If the surface is perfectly glossy (exhibiting specular “interface” reflectance that depends on incidence angle, and that is characteristic of light passing from air to a smooth surface), laboratory AM1.5GV SR will underestimate reference AM1.5GV SR by 0.002 (nonselective white) to 0.015 (nonselective black). Measurements of the magnitude of the specular component reflected by representative wall products suggest that this underestimation will not exceed 0.01.

4.2.2 Reflectometer

We will measure laboratory AM1.5GV solar reflectance following ASTM C1549-09(2014) (Standard Test Method for Determination of Solar Reflectance Near Ambient Temperature Using a Portable Solar Reflectometer) (ASTM 2009) with a Devices & Services Solar Spectrum Reflectometer, version 6 (Figure 3), once the AM1.5GV solar spectral irradiance is added to its firmware. Three non-overlapping measurement spots will be chosen along a diagonal spanning the exposure face of each specimen.

One advantage of measuring solar reflectance with a reflectometer, rather than with a spectrometer, is that the reflectometer can be kept clean simply by inverting the measurement head to face down. The instrument will be calibrated and operated in this inverted configuration.

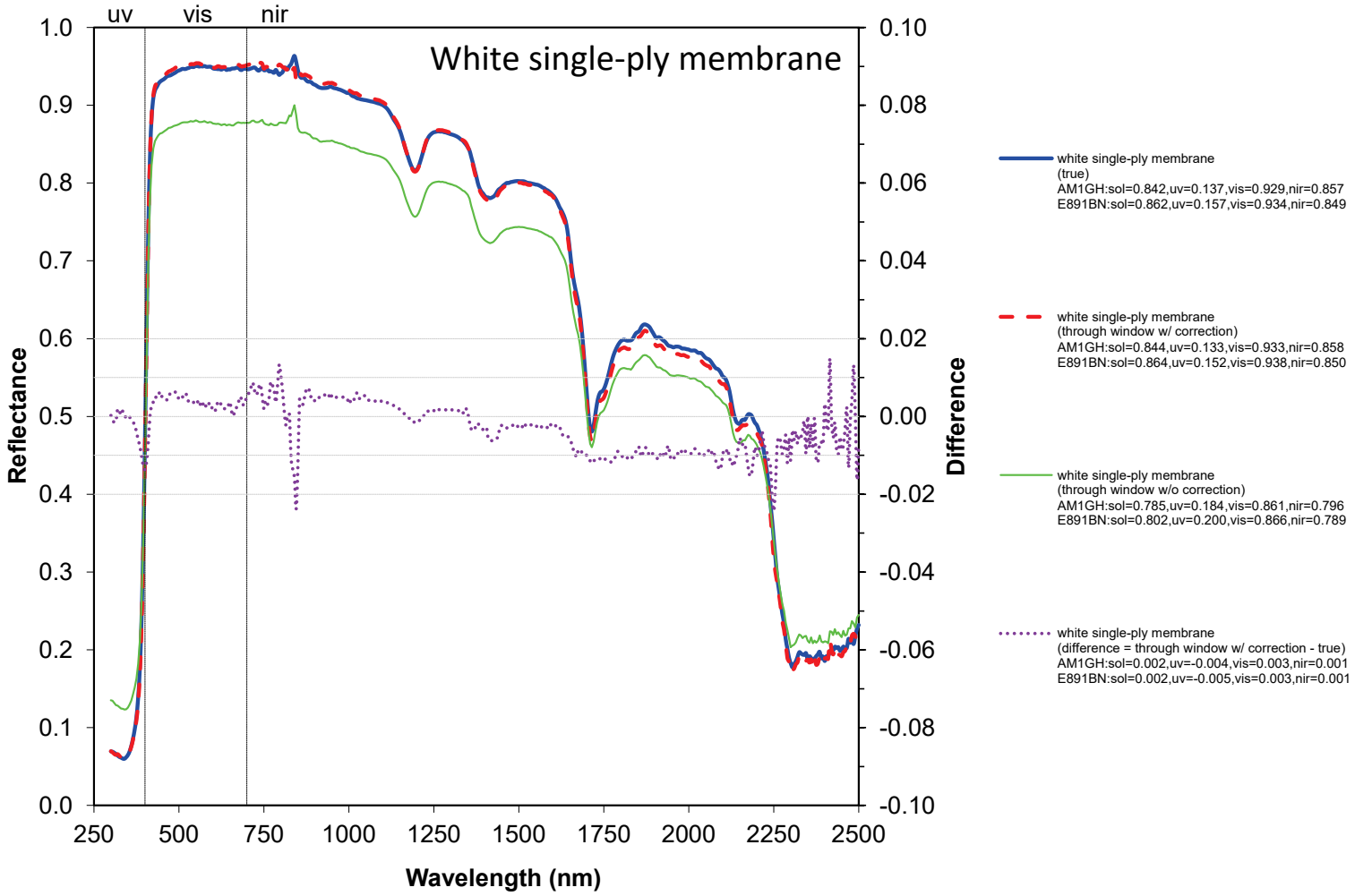

(a)

Figure 2. Solar spectral reflectances (300 – 2,500 nm @ 5 nm) of a variety of roofing products, including (a) white single-ply membrane, (b) blue single-ply membrane, (c) white painted metal (factory applied), (d) red clay tile, (e) cool green painted metal (factory applied), and (f) clear acrylic resin-coated Zincalume steel. The spectral reflectance of each specimen is shown (i) measured without a window

("true"); (ii) measured through a window, then corrected; and (iii) measured through a window, uncorrected. The difference (corrected – true) is also shown.

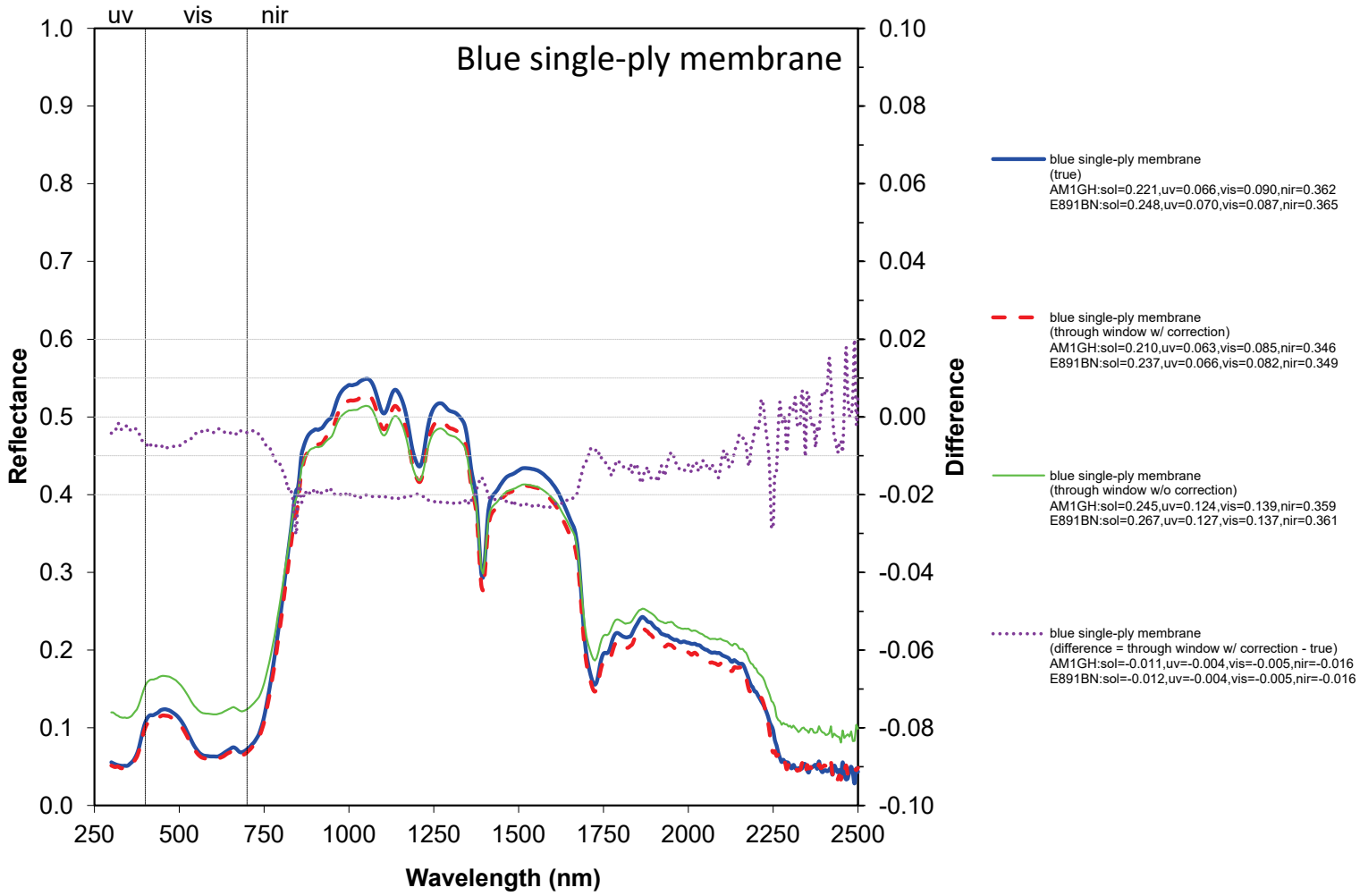

(b)

sol=300-2500 nm; uv=300-400 nm; vis=400-700nm; nir=700-2500 nm

Figure 2 (continued)

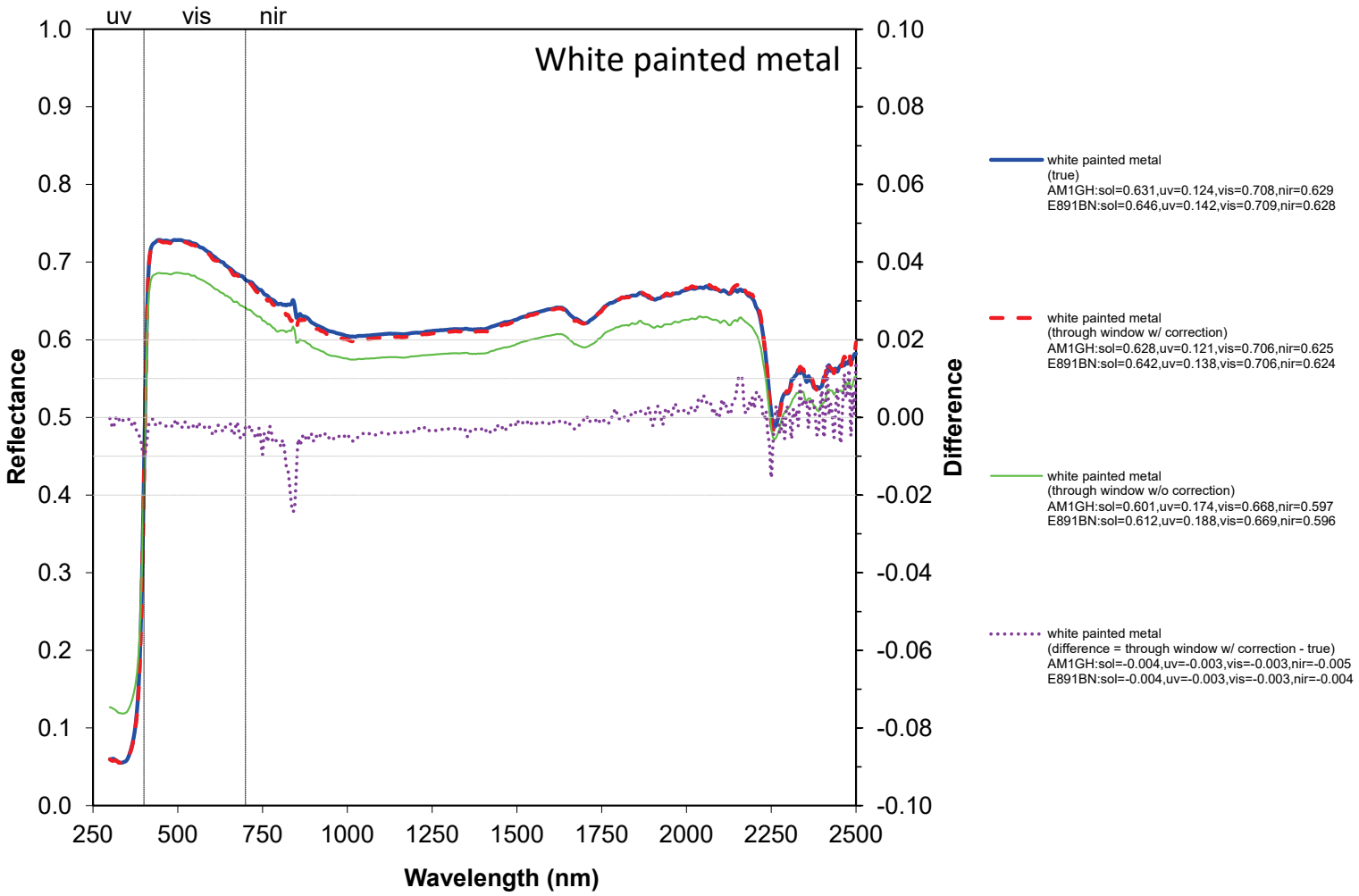

(c)

sol=300-2500 nm; uv=300-400 nm; vis=400-700nm; nir=700-2500 nm

Figure 2 (continued)

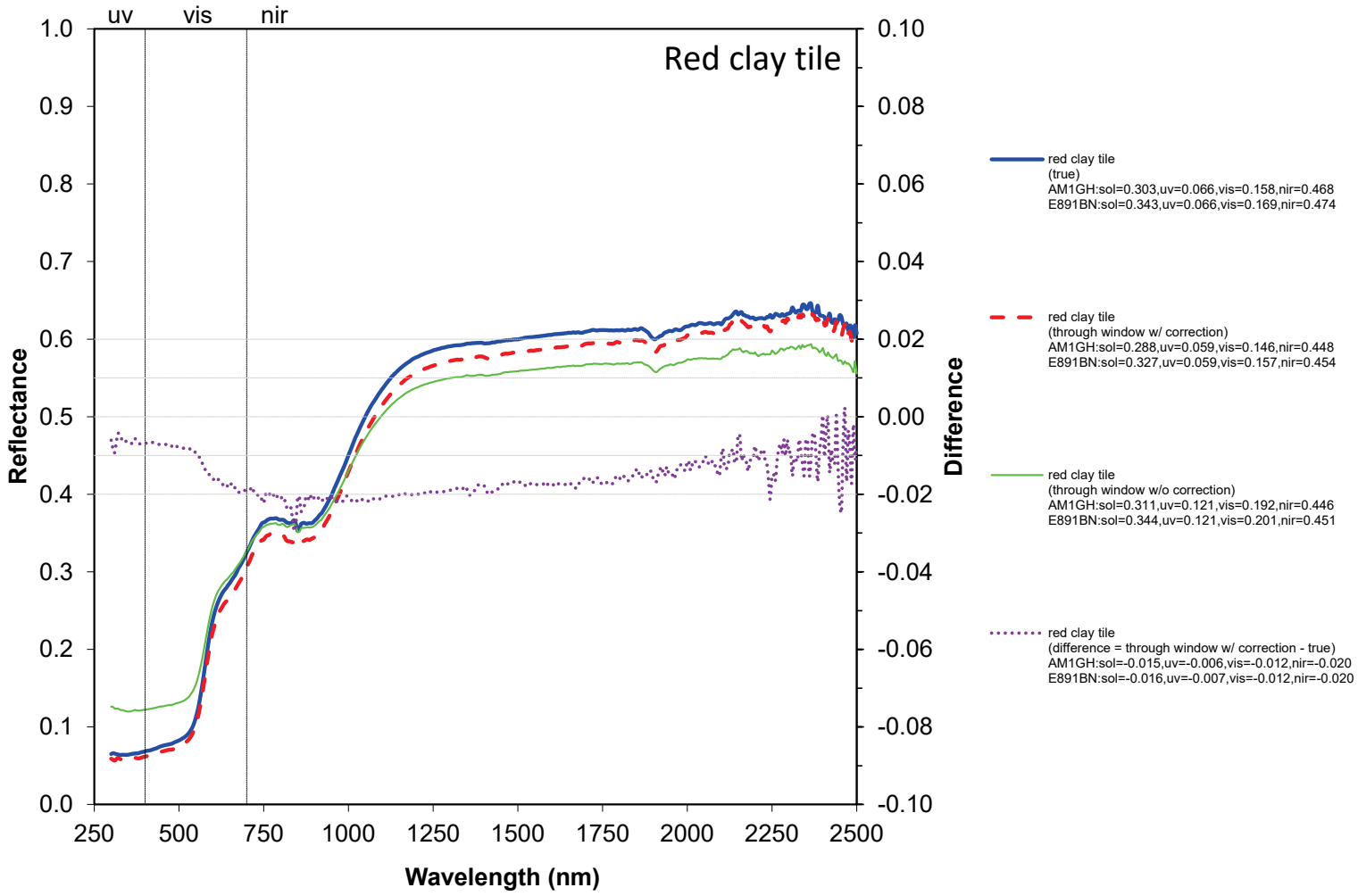

(d)

sol=300-2500 nm; uv=300-400 nm; vis=400-700nm; nir=700-2500 nm

Figure 2 (continued)

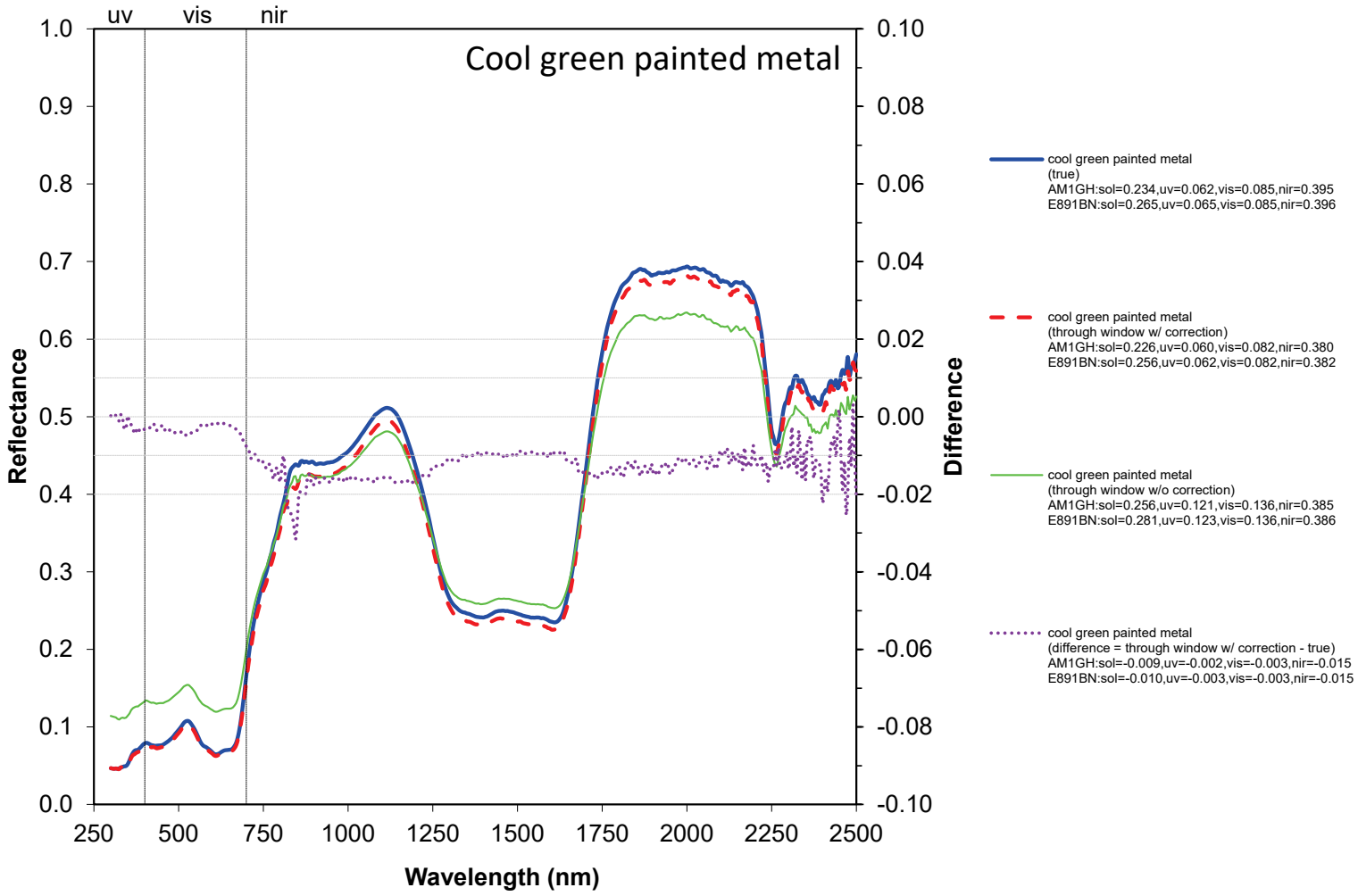

(e)

Figure 2 (continued)

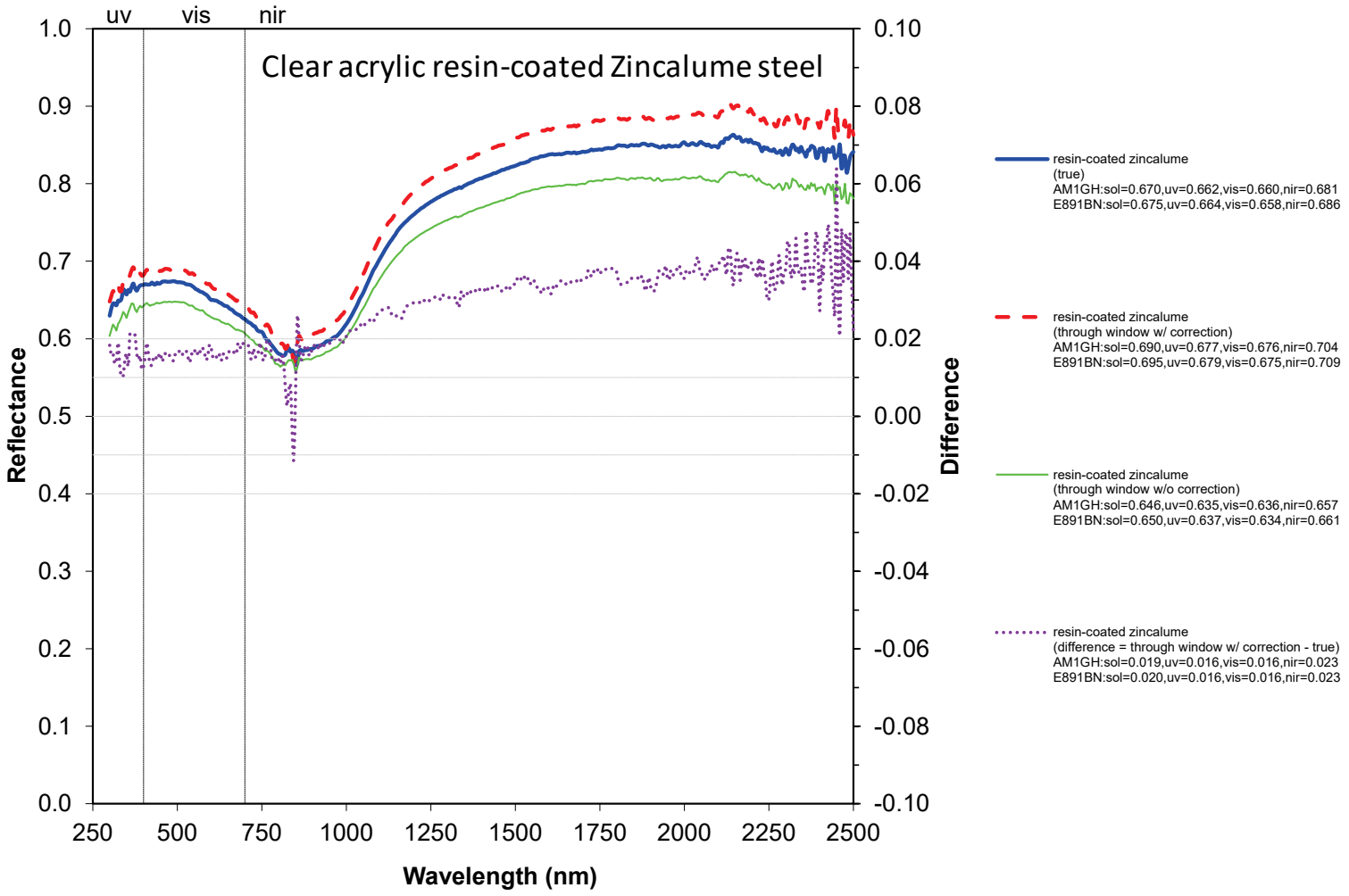

(f)

Figure 2 (continued)

4.2.3 Pyranometer

We do not at this time plan to measure wall solar reflectance with a pyranometer, because there does not yet exist a version of ASTM E1918 (Standard Test Method for Measuring Solar Reflectance of Horizontal and Low-Sloped Surfaces in the Field) (ASTM 2006) suitable for walls. Supporting, orienting, and operating a pyranometer half a meter away from a large wall surface (at least 4 m in diameter) may be tricky.

4.3 Color

CIELAB color coordinates can be calculated from solar spectral reflectance measured with a UV-VIS-NIR spectrometer, since the spectrum needed to compute color (380 – 760 nm) following ASTM E308 is a subset of the solar spectrum (300 – 2,500 nm). Another option is to use a dedicated colorimeter, such as a MiniScan EZ 4500L Spectrophotometer.

4.4 Effective solar reflectance

The measurement of effective solar reflectance is detailed by Levinson et al. (2017). A preprint of this article is presented in our Task 5.2 report: *Development of fluorescent cool pigments.*

4.5 Solar retroreflectance

The characterization of solar retroreflectance is detailed in our Task 5.3 report: *Development of retroreflective materials.*

Figure 3. Devices & Services Solar Spectrum Reflectometer, Model SSR-ER, version 6, operated with its measurement head inverted.

Figure 4. Devices & Services Portable Emissometer, Model AE1, and a multimeter.

4.6 Thermal emittance

Hemispherical thermal emittance will be measured using a Devices & Services Emissometer Model AE1 (Figure 4) with the ADP Port Adapter accessory. Specimens with high thermal conductance (> 1100 W/m²·K),[1] such as bare or painted metal panels, will be measured per ASTM C1371-15 (Standard Test Method for Determination of Emittance of Materials Near Room Temperature Using Portable Emissometers) (ASTM 2015a). All other specimens will be measured per the "Slide Method" described in Devices & Services technical note TN11-2 (Moore 2011).

The instrument will be calibrated, maintained, and operated according to manufacturer instructions, except in specific situations where doing so will irreversibly damage specimens. For example, some steps as described in the "Slide Method" technical note (such as the use of a fan, and the "sliding" action of the measurement head) will need to be modified slightly in order to minimize disturbance to field-exposed specimens.

4.7 Initial and aged solar reflectance and thermal emittance

The variation with time of the radiative properties of wall products will be measured in accordance with the practices described in the section "Natural exposure study protocol".

---

[1] Thermal conductance is the reciprocal of thermal resistance. Hence, ASTM C1371 applies only to specimens with low thermal resistance (< 0.00091 m²·K/W, or 0.0052 ft²·°F·h/BTU).

4.8 Solar reflectance loss and thermal emittance gain

Measured values of initial and aged AM1.5GV solar reflectance will be used to calculate solar reflectance loss. Similarly, measured values of initial and aged hemispherical thermal emittance will be used to calculate thermal emittance gain.

4.9 Soiling resistance

Measured values of initial and aged AM1.5GV solar reflectance will be used to calculate relative soiling resistance in accordance with Eq. (3), and to calculate absolute soiling resistance in accordance with Eq. (4).

4.10 Hydrophilicity/hydrophobicity

Surface hydrophilicity or hydrophobicity will be determined by measuring water contact angle with a goniometer, in accordance with the static sessile drop method (Figure 5). This method determines the surface energy of a surface by placing a droplet of a liquid (water) of a known surface energy. The contact angle between the drop and the surface is measured under static conditions in which the drop is sitting on the surface, rather than rolling over it. It has been found to be the most appropriate method to quantify the contact angle of porous materials such as soils and sediments (Shang et al. 2008).

Static water contact angle will be measured via the sessile drop technique using a simple manually-operated setup. It consists of a point-and-shoot digital camera with focusing lens, a micrometer syringe, and an adjustable-height horizontal specimen mounting stage backlit by a diffuse light source. The camera is positioned such that it will view the sessile drop at a slight downward angle; this facilitates visual determination of the horizon in the resultant photograph.

A droplet of deionized water (of fixed volume on the order of a few microliters) is formed at the syringe tip and subsequently deposited onto the specimen surface very carefully. It is important that the droplet does not “fall” onto the specimen as this will distort the drop shape. The sessile drop is then photographed twice in order to capture any changes in drop shape over time – the first will be taken at 2 seconds following deposition, and the second will be taken at 30 seconds following deposition.

A free drop shape analysis tool, the "LBADSA" ImageJ plug-in (http://bigwww.epfl.ch/demo/dropanalysis) developed by Stalder et al. (2010), will be used to determine the contact angle from the drop photographs. If a drop is not symmetric, both the "left" and the "right" contact angles will be measured and recorded. Each specimen will be characterized by measurements of at least three drops positioned along a diagonal spanning the exposure face.

5 Natural exposure study protocol

5.1 Specimen selection

We selected 69 wall products from 10 partners to include in the natural exposure campaign (Figure 6). This set of products covers several types of wall materials and coatings typically

(a)

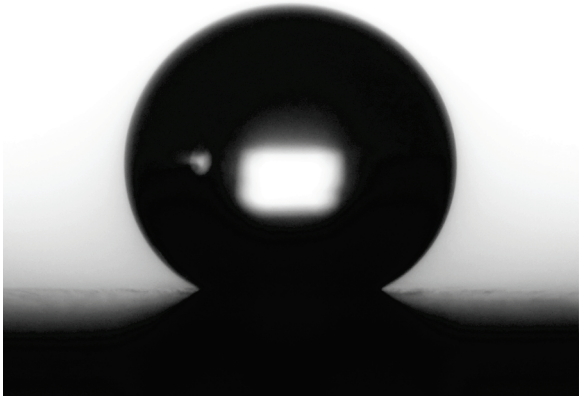

(b)

Figure 5. Sessile drop photographs produced by LBNL set-up, showing (a) a hydrophilic surface, and (b) a hydrophobic surface.

used in residential and commercial construction. It includes low-, medium-, and high-albedo products, as well as both conventional and self-cleaning products.

5.2 Specimen preparation

Partners were asked to prepare 100 replicate specimens of each product, each approximately 10 cm × 10 cm (4″ × 4″). To ensure their uniformity, we asked that these replicate specimens be cut from or produced in the same batch. Field-applied coatings were applied to appropriate substrates according to manufacturer specifications. Wood specimens were sealed on all sides in order to prevent situations where unrepresentative substrate degradation could impact true coating performance. The different categories are presented in the chart shown in Figure 6.

5.3 Specimen use

Of the 100 replicate specimens per product, 30 will be used in the initial 2 year exposure campaign in California. Exposing 10 specimens per product at each of the three California sites (Berkeley, Fresno, Los Angeles) will allow for retrieval of one specimen per product per site at the end of each of eight quarters. The remaining two specimens are spares that can be used in case of damage, or to extend the duration of exposure.

Another 18 specimens per product may be used in a parallel project to initiate a 5 year campaign at the three U.S. natural exposure sites (near Phoenix, AZ; Miami, FL, and Cleveland,

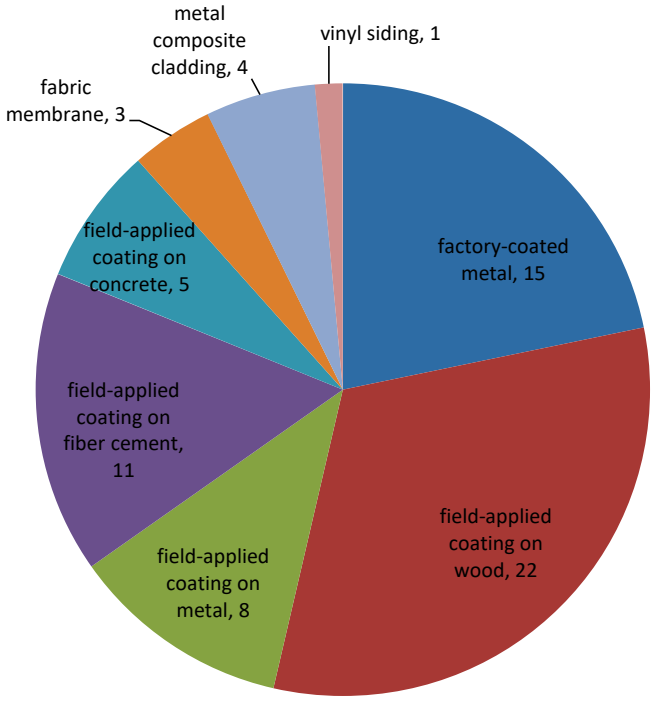

Figure 6. Distribution of cool wall products included in this study.

OH) used by the Cool Roof Rating Council for roof product rating. Exposing six specimens per product at each site will permit five annual retrievals, and provide one spare in case of damage.

Remaining specimens will be used for various laboratory tests at LBNL, including the potential development of a lab aging practice for wall products.

5.4 Specimen tracking

All information collected for each specimen—including product make and model, product manufacturer, specimen status, condition, solar reflectance, thermal emittance, and water contact angle—will be centralized and maintained in a database. Specimens are identified by a barcode asset tag attached to the back face, with a unique ID code of the format "CWXXYY", where "XX" is a 2-digit identifier (01-69) of product, and "YY" is a 2-digit identifier (00-99) of specimen replicate number (Figure 7).

5.5 Exposure practice at California sites

The wall product specimens will undergo direct natural exposure at three California locations: Lawrence Berkeley National Laboratory, in Berkeley; a PPG facility, in Fresno, and the University of Southern California, in Los Angeles. Experimental protocol will follow, as much as is possible, ASTM G7/G7M-13 (Standard Practice for Atmospheric Environmental Exposure Testing of Nonmetallic Materials) (ASTM 2013). To appropriately represent the product application, specimens will be exposed in a vertical orientation (90°) and backed by untreated marine-grade plywood. Since solar-reflective surfaces are expected to yield greatest energy savings when applied to east and west walls, and greatest peak power demand savings when applied to west

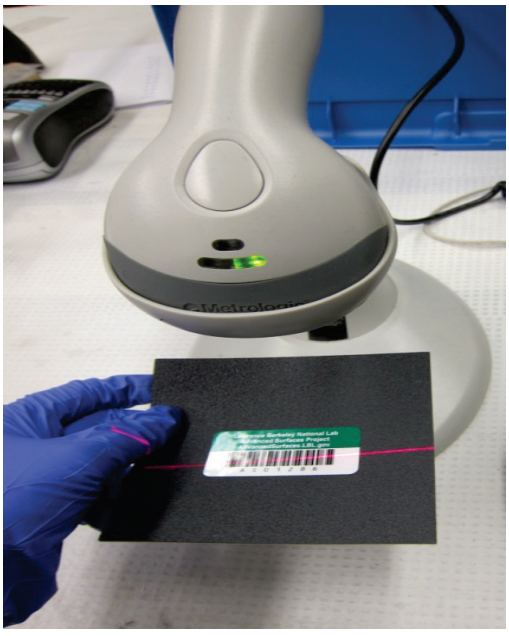

Figure 7. Example of label containing barcode (attached to back of specimen), being processed with a barcode reader.

walls, exposed specimens will face west.

Specimens will be mounted on custom-built exposure racks composed of 12 to 13 staggered rows of galvanized steel sheet metal specimen holders attached to a Unistrut frame (Figure 8). Staggering minimizes potential runoff cross-contamination between rows. Five drainage holes evenly spaced along the bottom of the specimen holders prevent water from collecting in the bottom jaws of the holders.

Each 2.1 m (7') long holder can hold up to 21 specimens, and thus can accommodate the full set of replicate specimens (10 each) for two products. This simplifies quarterly specimen retrieval, in which on-site staff need only slide one specimen from each end of the row.

5.6 Specimen characterization

At each of the eight quarters, one specimen per product per California site will be removed from the rack and sent to LBNL for characterization. The physical condition, radiative properties, and hydrophilicity/hydrophobicity of these specimens will be characterized with photographs, and with measurements of solar spectral reflectance, solar reflectance, thermal emittance, and water contact angle.

Because most measurements will to some degree disturb the soiling on naturally-exposed specimens, it will be important to order the measurement tasks starting from those with the least disturbance potential to those with the highest. The specimens will first be photographed, and then subjected to reflectometer and spectrometer measurements. Thermal emittance and water contact angle will be measured last. Retrieved specimens will be stored at LBNL after characterization.

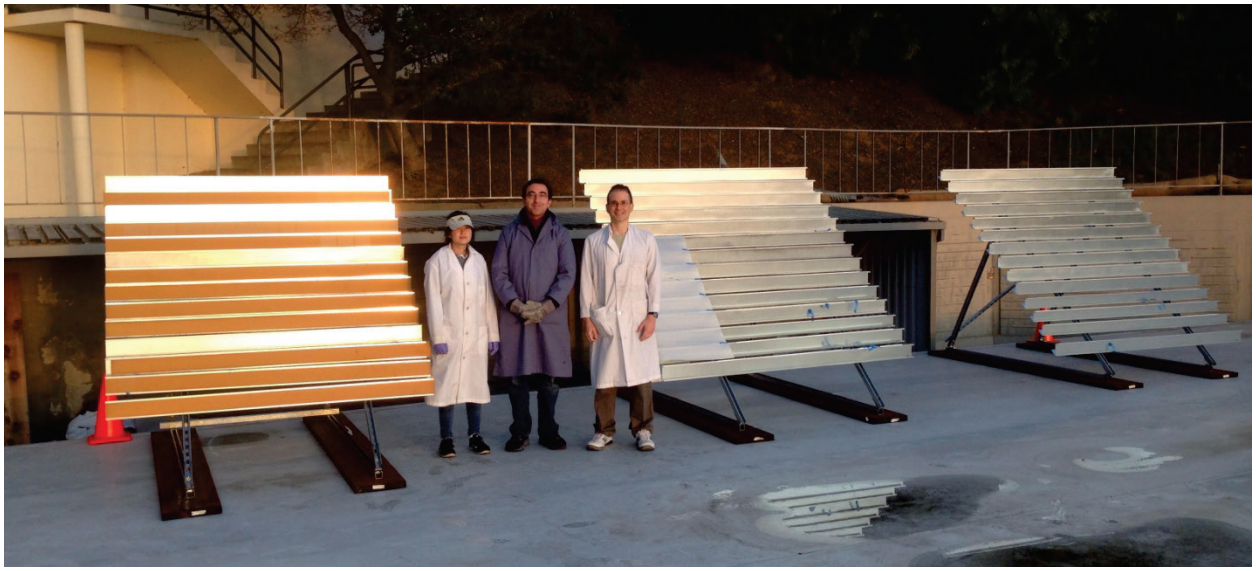

Figure 8. LBNL-designed wall product exposure racks freshly installed on a roof at Lawrence Berkeley National Laboratory (Berkeley, CA).

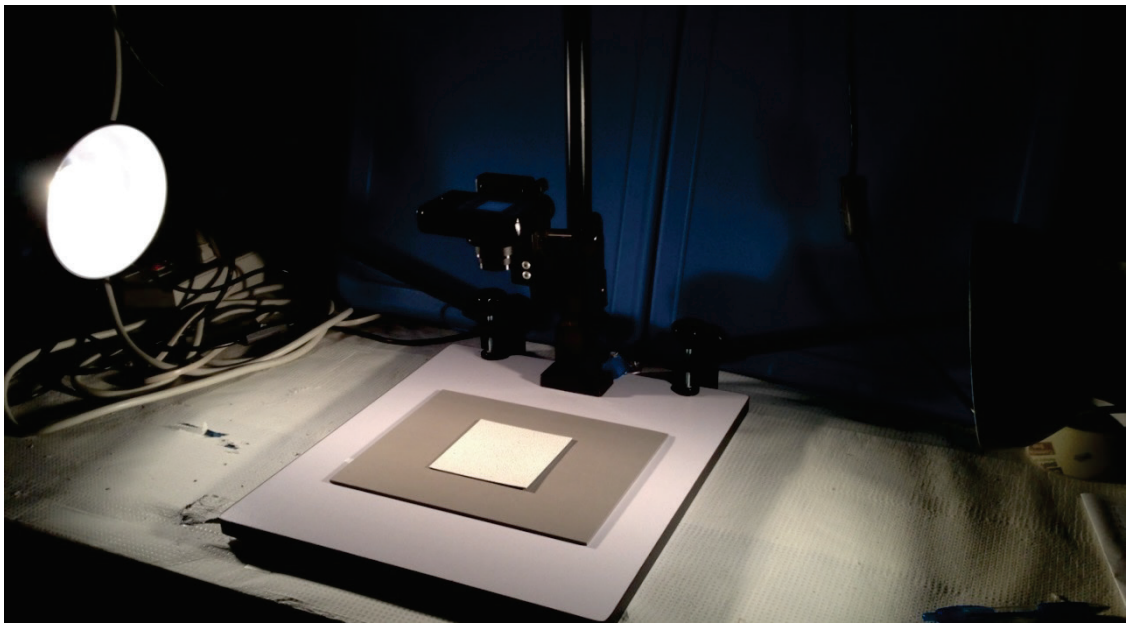

The following information will be gathered before exposure, and following quarterly specimen retrieval.

5.6.1 Image

Specimens will be photographed using a point-and-shoot digital camera mounted on a copy stand set-up that provides reproducible lighting conditions. A gray card placed in background will be helpful for white balance (Figure 9).

Figure 9. Photo copy table used to prepare specimen photos.

5.6.2 Solar spectral reflectance

Solar spectral reflectance will be measured with a UV-VIS-NIR spectrometer, as described in the Methods subsection “Solar spectral reflectance”.

Solar reflectance

Solar reflectance will be measured with a UV-VIS-NIR spectrometer, and—once the reflectometer firmware is upgraded to include the AM1.5GV solar spectral irradiance—with a Devices & Services Solar Spectrum Reflectometer. Both practices are detailed in the Methods subsection “Solar reflectance”.

5.6.3 Thermal emittance

Thermal emittance will be measured with a Devices & Services Portable Emissometer, as described in the Methods subsection “Thermal emittance”.

5.6.4 Water contact angle

Water contact angle will be measured with our custom apparatus as described in the Methods subsection “Hydrophilicity/hydrophobicity”.

5.7 Specimen storage

Because it is necessary to preserve specimen condition prior to and after measurement, each specimen will be enclosed in its own glassine paper sleeve when not undergoing exposure or measurement (Figure 10). Glassine paper was chosen for the sleeve material as it is archival-grade, non-reactive, moisture-resistant, not prone to static buildup, and semi-transparent. Storing specimens using this method prevents contamination of clean specimens as well as accidental “cleaning” of field-exposed specimens. Any debris fall-off from a field-exposed specimen will be saved by collecting the debris inside the specimen’s glassine paper sleeve. For this reason, sleeves will not be interchanged between specimens, and any damaged sleeves will be replaced accordingly.

For long periods of storage, the specimens (each inside a glassine sleeve) will additionally be placed inside a rigid waterproof secondary container. This is especially important since the glassine sleeves protecting the specimens are water-resistant, but not waterproof.

5.8 Specimen handling

Specimens need to be handled carefully in order to limit any disturbance to their condition. This involves gentle handling of both the specimen itself and its corresponding protective sleeve. The exposure face of the specimen must never be touched, scraped, or otherwise artificially contaminated by agents not representative of the exposure environment or time period. While inserting or removing specimens from their glassine sleeves, care will be taken to prevent the sleeve material from brushing against the exposure face. Likewise, the specimens will only be gripped along the side and back faces.

With field-exposed specimens there is a risk that rough handling will dislodge soiling debris that has collected on the exposure face. For this reason, it will be important to avoid violently agitating or inverting field-exposed specimens. Additionally, careful attention will be needed while specimens are being removed from the exposure racks to ensure that no damage or contamination occurs during this process. Once removed from the exposure environment and placed into glassine sleeves, these field-exposed specimens will not be handled in environments with significant levels of dust or drafts.

Many of the characterization measurements require direct contact between an instrument sample port and the specimen exposure face. In order to limit the degree of disturbance or contamination to both the specimen and the instrument, it will be necessary to clean the sample port between measurements, as well as prevent any static buildup on surfaces that come in close contact to the specimen.

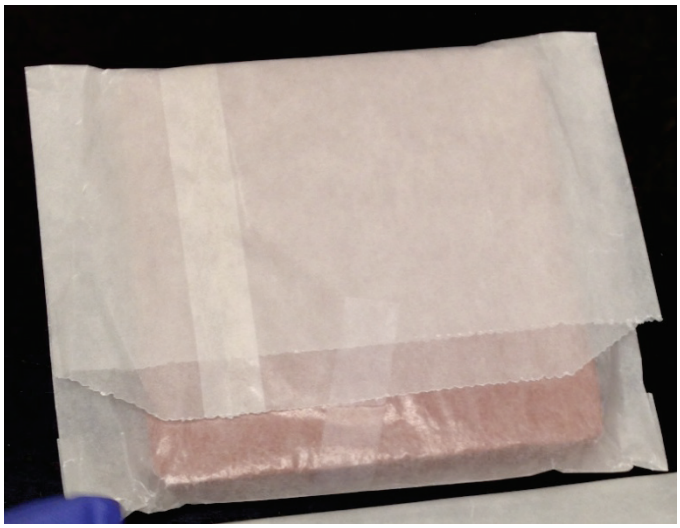

Figure 10. Specimen inside a glassine sleeve, which has been folded and taped closed.

5.9 Specimen packaging for transportation

While preparing specimens for long-distance transit via any of the typical carrier services, it is important to keep in mind that packages will be handled by personnel with no personal stake in this project. The many ways the integrity of specimens can be compromised during this process include physical damage to the specimen itself (as in breaking, chipping, scratching, or warping); disturbance of accumulated soiling; and in-package aging. Physical damage and disturbance of accumulated soiling can occur if specimens are allowed to shift around violently inside the secondary container, and/or if there is insufficient padding. In-package aging can occur if the specimens are packaged while “wet” (will leach moisture to surroundings under ambient conditions) or if the specimens become wet when package is exposed to heavy rains during transit. One specimen could soil another if packed in the same sleeve, or if a sleeve tears during transport and storage.

A proper packaging protocol will incorporate strategies that protect against the aforementioned causes of specimen damage. It will also incorporate only robust materials that will not fail during transit. Materials found to be robust include cardboard, bubble wrap, foam, and packaging tape. Materials found to be insufficient include rubber bands and copy paper.

The following describes a packaging protocol that has worked well for LBNL in the past. Each specimen is first inspected and determined to be sufficiently dry before it can be placed inside a clean glassine sleeve. The sleeve is then taped or folded over in some way to prevent the specimen inside from sliding around freely. Sleeved specimens are then arranged into a small stack, where sleeved specimens are separated from each other by buffer layers of cardboard, bubble wrap, or foam sheeting (Figure 11). Any flexible or fragile sleeved specimens are flanked by stiff material to preserve their shape. The stack of sleeved specimens is then bound tightly together such that individual specimens cannot independently move. These sleeved-specimen bundles can then be placed into a sturdy cardboard box where any voids are adequately filled with foam, bubble wrap, or air cushions. If it is expected that the box will contact water during transit, then these sleeved-specimen bundles should be wrapped in some water-resistant barrier.

Figure 11. Stacks of sleeved specimens.

6 Summary

We have developed and presented metrics and methods to characterize the solar spectral reflectance, solar reflectance, effective solar reflectance, solar retroreflectance, color, thermal emittance, soiling resistance, and hydrophilicity/hydrophobicity of wall products. We have also developed and presented a protocol for the natural exposure of wall products and California, with possible extension to three U.S. sites outside the state.

References

ASTM. 2006. ASTM E1918-06: Standard Test Method for Measuring Solar Reflectance of Horizontal and Low-Sloped Surfaces in the Field. ASTM International. http://www.astm.org/Standards/E1918.htm

ASTM. 2009. ASTM C1549-09(2014): Standard Test Method for Determination of Solar Reflectance Near Ambient Temperature Using a Portable Solar Reflectometer. http://www.astm.org/Standards/C1549.htm

ASTM. 2011. ASTM E1980-11: Standard Practice for Calculating Solar Reflectance Index of Horizontal and Low-Sloped Opaque Surfaces. ASTM International. http://www.astm.org/Standards/E1980.htm

ASTM. 2012. ASTM E903-12: Standard Test Method for Solar Absorptance, Reflectance, and Transmittance of Materials Using Integrating Sphere. ASTM International. http://www.astm.org/Standards/E903.htm

ASTM. 2013. ASTM G7/G7M-13: Standard Practice for Atmospheric Environmental Exposure Testing of Nonmetallic Materials. ASTM International. http://www.astm.org/Standards/G7.htm

ASTM. 2014. ASTM G197-14: Standard Table for Reference Solar Spectral Distributions: Direct and Diffuse on 20˚ Tilted and Vertical Surfaces. ASTM International. http://www.astm.org/Standards/G197.htm

ASTM. 2015a. ASTM C1371-15: Standard Test Method for Determination of Emittance of Materials Near Room Temperature Using Portable Emissometers. ASTM International. http://www.astm.org/Standards/C1371.htm

ASTM. 2015b. ASTM D7897-15: Standard Practice for Laboratory Soiling and Weathering of Roofing Materials to Simulate Effects of Natural Exposure on Solar Reflectance and Thermal Emittance. ASTM International. http://www.astm.org/Standards/D7897.htm

ASTM. 2015c. ASTM E308-15: Standard Practice for Computing the Colors of Objects by Using the CIE System. ASTM International. http://www.astm.org/Standards/E308.htm

Chabas A, Alfaro S, Lombardo T, Verney-Carron A, Da Silva E. Triquet S, Cachier H, Leroy E. 2014. Long term exposure of self-cleaning and reference glass in an urban environment: A comparative assessment. *Building and Environment* 79, 57-65.

Gueymard C. 2006. Simple Model of the Atmospheric Radiative Transfer of Sunshine (SMARTS) 2.9.5. http://www.nrel.gov/rredc/smarts

Levinson R, Akbari H, Berdahl P. 2010a. Measuring solar reflectance—Part I: defining a metric that accurately predicts solar heat gain. *Solar Energy* 84, 1717-1744.

Levinson R, Akbari H, Berdahl P. 2010b. Measuring solar reflectance—Part II: review of practical methods. *Solar Energy* 84, 1745-1759.

Levinson R, Chen S, Ferrari C, Berdahl P, Slack J. 2017. Methods and instrumentation to measure the effective solar reflectance of fluorescent cool surfaces. *Energy & Buildings* 152, 752-765. http://dx.doi.org/10.1016/j.enbuild.2016.11.007

Moore C. 2011. Model AE1 Emittance Measurements using a Port Adapter, Model AE-ADP. Technical Note TN11-2, Devices & Services Company, Dallas, TX. http://www.devicesandservices.com/TechNotes/TN11-2.pdf

Schaeffer DA, Polizos G, Smith DB, Lee DF, Hunter SR, Datskos PG. 2015. Optically transparent and environmentally durable superhydrophobic coating based on functionalized SiO_2 nanoparticles. *Nanotechnology* 26 (5), 055602. http://dx.doi.org/10.1088/0957-4484/26/5/055602

Shang J, Flury M, Harsh JB, Zollars RL. 2008. Comparison of different methods to measure contact angles of soil colloids. *Journal of Colloid and Interface Science* 328, 299-307.

Sleiman M, Ban-Weiss G, Gilbert HE, Francois D, Berdahl P, Kirchstetter TW, Destaillats H, Levinson R. 2011. Soiling of building envelope surfaces and its effect on solar reflectance—Part I: Analysis of roofing product databases. *Solar Energy Materials & Solar Cells* 95, 3385-3399.

Stalder AF, Melchior T, Müller M, Sage D, Blu T, Unser M. 2010. Low-bond axisymmetric drop shape analysis for surface tension and contact angle measurements of sessile drops. *Colloids and Surfaces A: Physicochemical and Engineering Aspects* 364(1-3), 72-81.

Task Report Appendix A: Development of a solar reflectance metric for walls

Motivation

If the reflectance of a surface is both "matte" (invariant with incident angle) and nonselective (invariant with wavelength), its solar reflectance will be constant. Otherwise, its solar reflectance can vary with the geometry (angular distribution) and/or spectral power distribution (power per unit wavelength, by wavelength) of incident sunlight, each of which depend on the position of the sun, the orientation of the surface, sky conditions, shading, and (unless the surface is horizontal) ground reflectance.

Spectral and solar reflectance can vary strongly with incidence angle if a surface is "glossy" (exhibits a specular "interface" reflectance characteristic of light passing from air to a smooth surface) and has low reflectance at near-normal incidence. For example, a smooth black surface may reflect 4% of light incident near normal, but 20% of light incident 70° from normal. This is evident from the images, or glare, that can be seen in smooth black surfaces when viewed from large incidence angle.

Solar reflectance can vary strongly with solar spectral irradiance if the surface's reflectance changes substantially by wavelength. For example, Levinson et al. (2010a) calculated that an ideal matte cool black horizontal surface with 0.04 reflectance in the UV and visible spectra (300 – 700 nm), and 0.90 reflectance in the NIR spectrum (700 – 2,500 nm), would exhibit a solar reflectance of 0.46 in full sun (solar irradiance 49% NIR), but only 0.27 in full shade (solar irradiance 17% NIR).

Methodology and intermediate results

The article by Levinson et al. (2010a) developed a solar reflectance metric suitable for predicting the solar heat gain of a horizontal surface, such as a flat roof or pavement, or an axisymmetric surface, such as a conical roof or the entire curved side wall of a cylinder. That study chose to evaluate solar conditions at the time of peak irradiance. That maximizes the accuracy of solar reflectance when the sun is strong, and tends to reduce errors in solar heat gain. We follow their approach to select a solar reflectance metric suited to flat walls. To wit:

1. Using the NREL SMARTS2 tool (Gueymard 2006), we calculate global, beam (direct), and diffuse (sky + ground) solar spectral irradiances under the ASTM G197 sky and ground conditions as a function of solar altitude angle and surface solar azimuth angle (solar azimuth angle – surface azimuth angle). The spectral irradiance simulation process is detailed in Section 5.1 of Levinson et al. (2010a).

2. From these spectral irradiances we calculate global solar irradiance, beam solar irradiance, diffuse solar irradiance, diffuse fraction of global solar irradiance, and NIR fraction of global solar irradiance as a function of solar position (Figure 12).

3. We determine that under G197 sky and ground conditions, a vertical surface experiences peak global solar irradiance at when the sun altitude angle is 32° and the surface solar azimuth angle is zero (surface faces the sun). This solar position is marked "P" (for peak) in Figure 12.

4. Table 1 shows that the magnitude, NIR fraction, and diffuse fraction of the peak global solar irradiance are close to those specified by ASTM G197 for an air mass 1.5 global solar irradiance on a sun-facing vertical surface (solar altitude 42°, surface solar zenith angle zero; marked "G", for G197, in Figure 12). Since the G197 air mass 1.5 global vertical (AM1.5GV) irradiance well matches the peak global solar irradiance, and is already published as an ASTM standard, we use the solar position and solar spectral irradiance associated with G197 AM1.5GV as our conditions for evaluating "reference" global solar reluctances.

5. For glossy and matte versions of several ideal surfaces (nonselective black with near-normal UV and visible reflectance r_V=0.04, and near-normal NIR reflectance r_N=0.04; nonselective gray with r_V=r_N=0.20; nonselective white with r_V=r_N=0.90; selective black with r_V=0.04, r_V=0.90; and selective gray with r_V=0.20, r_V=0.90), we calculate global solar reflectance as a function of solar position. The reflectance calculation process is detailed in Section 5.2 of Levinson et al. (2010a). Figure 13 shows the results for all surfaces that are glossy, selective, or both. (Global solar reflectance is invariant for a matte, nonselective surface.)

6. Using the NREL SOLPOS tool (https://www.nrel.gov/midc/solpos/solpos.html), we calculate the solar path (altitude and azimuth angles by time of day) the 21st day of each month, including Mar 21 (spring equinox), Jun 21 (summer solstice), Sep 21 (fall equinox), and Dec 21 (winter solstice), at latitudes 25°N (just south of Miami, FL), 37°N (mid-latitudes of mainland U.S. and California), and 45°N (Portland, OR). Solar paths at latitude 37°N are shown in Figure 14.

7. At each latitude (25°N, 37°N, 45°N), on each date (Mar 21, Jun 21, Sep 21, Dec 21), and for each cardinal wall direction (east, west, south, and north), we calculate the variation with time of day of the global solar irradiance; NIR and diffuse fractions of global solar irradiance; underestimation of global solar reflectance by reference solar reflectance; and overestimation of solar heat gain induced by substituting reference reflectance for global solar reflectance. Figure 15 shows these results at latitude 37°N. Reflectance underestimation and solar heat gain overestimation for the gray surfaces are omitted to simplify the graphs, but are similar to those for the black surfaces.

8. We calculate for each latitude, date, and wall orientation the underestimation of daily reflectance (fraction of daily solar irradiation reflected) by reference solar reflectance, and the overestimation of daily solar heat gain (daily solar irradiation absorbed) by induced by substituting reference reflectance for global solar reflectance. Table 2 shows these results at latitude 37°N.

9. Since the cooling energy savings and heating energy penalties associated with raising wall solar reflectance scale with increase in solar reflectance, we calculate the extent to which substituting reference reflectance for global solar reflectance will overestimate true rises in summer (Jun/Jul/Aug) and winter (Dec/Jan/Feb) solar reflectances. Table 3 shows results for six scenarios in which nonselective black or gray surfaces are upgraded to selective black, selective gray, or nonselective white surfaces. It omits cases in which a matte nonselective is upgraded to another matter nonselective surface, because the reflectances of matte nonselective surfaces are constant.

We extended the earlier study in at least one regard. To assess whether wall products tend to be matte or glossy, we measured the specular component of the AM1GH solar reflectance of 14 different wall products, and of 6 reference materials, with a UV-VIS-NIR spectrometer (Table 4). The procedure was to (a) open the specular reflectance port of the spectrometer's integrating sphere; (b) calibrate the instrument; (c) measure $r_1(\lambda)$, the solar spectral reflectance excluding specular component, of each specimen; (d) close the port; (e) re-calibrate the instrument; and (f) measure total solar spectral reflectance, $r_2(\lambda)$, of each specimen. The specular component of solar spectral reflectance was calculated as $r_3(\lambda) = r_2(\lambda) - r_1(\lambda)$, and weighted with AM1GH solar spectral irradiance to obtain the specular component of solar reflectance. (The solar spectrum used to weight spectral irradiance is not particularly important in this assessment of glossiness.)

Discussion

Error in solar heat gain

There are three types of error when using a fixed reference reflectance to estimate solar heat gain: (A) those due to mismatch in spectral power distribution when a surface is selective, (B) those due to mismatch in incidence angle when a surface is not matte; and (C) those that result from a combination of A and B. Here we gauge each type of error for walls at latitude 37°N (mid-mainland US, mid-California) using results presented in Table 2.

The selective black ideal surface is highly selective, and more so than any real cool color. Therefore, we can use the fractional overestimation of wall daily solar heat gain for this surface to bound type A (spectral) errors. This error ranges from -5.2% (south) to +2.5% (east and west) on Jun 21; from -8.3% (north) to +9.0% (south) on Dec 21; and from -8.5% (north) to +4.1% (east and west) on Mar 21 and Sep 21. The magnitude (absolute value) of the type A error does not exceed 9% for any cardinal direction.

We can bound type B (angular) errors by considering a glossy nonselective black surface, which exhibits maximum variation of reflectance with incidence angle. This error ranges from +2.7% (east and west) to +19.2% (south) on Jun 21; from -0.1% (south) to +5.4% (east and west) on Dec 21; and from +3.0% (east and west) to +6.2% (south) on Mar 21 and Sep 21. The magnitude of the type B error does not exceed 5.4% for east and west walls, but on Jun 21 can reach 19.2% for a south wall.

It is more challenging to bound type C (spectral + angular) errors, because type A and type B errors for a glossy selective surface can have opposite signs. However, we will consider the range of errors in for the glossy selective black and glossy selective gray, choosing the largest values. This error ranges from +5.4% (east and west) to +13.3% (north) on Jun 21; from -4.7% (north) to +14.4% (east) on Dec 21; and from -4.9% (north) to +7.5% (east and west) on Mar 21 and Sep 21. For east and west walls, the magnitude of the type C error does not exceed 7.5% on Mar, Jun, or Sep 21, but can reach 14.4% on Dec 21. For north and south walls, the magnitude of the type C error can reach 12.6% (south) to 13.3% (north) in on Jun 21, but otherwise does not exceed 8.9%.

Error in solar reflectance rise

Substituting reference reflectance for actual reflectance can induce type A, B, and C errors in estimation of solar reflectance rise when making walls cooler. The following results are evaluated at latitude 37°N (Table 3).

We bound type A (spectral) errors using scenario (e), matte nonselective black to matte selective black. For east and west walls, the overestimation of reflectance rise is -2.9% in summer and -6.6% in winter. For south walls, the error is +5.1% in summer and -6.2% in winter. For north walls, the error is +1.1% in summer and +11.2% in winter.

We bound type B (angular) errors using scenario (a), glossy nonselective black to glossy nonselective white. For east and west walls, the overestimation of reflectance rise is +2.7% in summer and +4.6% in winter; for north and south walls, the error is small in summer (+0.7% to +4.0%), but large in winter (+10.8% to +16.3).

We bound type C (spectral + angular) errors using scenario (c), glossy nonselective black to glossy selective black. For east and west walls, the overestimation of reflectance rise is -0.5% in summer and -2.6% in winter. For south walls, the error is +23.1% in summer and -5.5% in winter. For north walls, the error is +13.2% in summer and +15.8% in winter.

Note that reflectance rise errors are usually a few percentage points lower or higher if substituting laboratory reflectance, rather than reference reflectance, for the true reflectance of a glossy surface, because for a glossy surface AM1.5GV reference reflectance (based on 42° incidence) can be up to 0.015 higher than AM1.5GV laboratory reflectance (based on near-normal incidence).

Applicability of AM1.5GV solar reflectance by wall orientation

East and west walls. The preceding analysis indicates that for east and west walls, the magnitude of type A (spectral) and type B (angular) errors in solar heat gain does not exceed 9%, and the magnitude of type A and type B errors in reflectance rise does not exceed 6.6%. The magnitude of Type C error in solar heat gain can reach 14.4% in on Dec 21, but the magnitude of type C error in reflectance rise does not exceed 2.6%. This suggests that the AM1.5GV solar reflectance is suited to east and west walls.

South walls. The preceding analysis indicates that for south walls, the magnitude of type A (spectral) error in solar heat gain does not exceed 9%, and the magnitude of type A error in reflectance rise does not exceed 6.2%. The magnitude of type B (angular) error in solar heat gain can reach 19.2% on Jun 21, and the magnitude of type B error in reflectance rise can reach 16.3% in summer. The magnitude of type C (spectral + angular) error in solar heat gain can reach 12.6% on Jun 21, and the magnitude of type C error in reflectance rise can reach 23.1% in summer. The low type A and large type B and C errors in summer reflectance rise suggest that the AM1.5GV solar reflectance is suited to matte, but not glossy, south walls.

North walls. The preceding analysis indicates that for north walls, the magnitude of type A error in solar heat gain does not exceed 9%, but the magnitude of type A (spectral) error reflectance rise can be reach 11.2% in summer. The magnitude of type B (angular) error in solar heat gain can reach 12.0% on Jun 21, and the magnitude of type B error in reflectance rise can reach 10.8% in winter. The magnitude of type C (spectral + angular) error in solar heat gain can reach 13.3% on Jun 21, and the magnitude of type C error in reflectance rise can reach 15.8% in winter. The large type A, B, and C errors in reflectance rise suggest that the AM1.5GV solar reflectance may not be suited to north walls.

However, two mitigating factors may increase the applicability of AM1.5GV solar reflectance to south and north walls. First, the ideal selective black and gray surfaces are much more selective than real cool colors. For example, a real selective gray is likely to have selectance $r_N - r_V = 0.60 - 0.20 = 0.40$, which is 43% smaller than that of the ideal selective gray ($r_N - r_V = 0.90 - 0.20 = 0.70$). This suggests that type A (spectral) errors may be about 40% smaller for actual wall products. Second, Table 4 shows that the measured solar specular reflectance from even the "glossiest" wall products tested (specimens 6-9, factory applied coatings on metal) did not exceed 0.026, which is 32% smaller than that observed from the truly "glossy" black-undercoated glass surface with a 0.042 solar specular reflectance. This suggests that type B (angular) errors may be about 1/3 smaller for actual wall products.

Conclusions

We recommend the use of the AM1.5GV solar reflectance metric for east and west walls. It may also be used for matte south walls. It is not well suited to fully glossy south walls, fully glossy north walls, or highly selective north walls.

Table 1. Comparison of solar angles, solar irradiances, and solar reflectances associated with two wall solar irradiances: (a) G197-14 AM1.5 global tilt irradiance on a sun-facing wall, and (b) peak global irradiance on a sun-facing wall.

	(a) G197	(b) peak	difference (G197 - peak)
solar azimuth angle (°)	0	0	0
solar altitude angle (°)	41.8	32.0	9.76
solar beam incidence angle (°)	41.8	32.0	9.76
global tilt irradiance (W/m²)	807.	837.	-30.0
diffuse tilt irradiance (W/m²)	143.	133.	10.9
beam tilt irradiance (W/m²)	664.	704.	-40.8
NIR fraction	0.533	0.547	-0.0134
diffuse fraction	0.178	0.158	0.0193
glossy nonselective black reflectance	0.0550	0.0499	0.00510
glossy nonselective gray reflectance	0.213	0.208	0.00425
glossy nonselective white reflectance	0.902	0.901	0.000532
glossy selective black reflectance	0.507	0.516	-0.00884
glossy selective gray reflectance	0.580	0.587	-0.00710
glossy selective white reflectance	0.450	0.435	0.0145
matte nonselective black reflectance	0.0400	0.0400	0
matte nonselective gray reflectance	0.200	0.200	0
matte nonselective white reflectance	0.900	0.900	0
matte selective black reflectance	0.499	0.510	-0.0116
matte selective gray reflectance	0.573	0.583	-0.00942
matte selective white reflectance	0.441	0.430	0.0116

Table 2. Laboratory, reference, and daily solar reflectances; daily solar heat gain; underestimations by reference reflectance of instantaneous and daily solar reflectances; and underestimations by reference reflectance of instantaneous and daily solar heat gains, shown for seven ideal wall surfaces at latitude 37°N. Values are reported on (a) Mar 21, (b) Jun 21, (c) Sep 21, and (d) Dec 21 for (i) east, (ii) west, (iii) south, and (iv) north walls.

(a–i) March, east							
	glossy nonselective black	glossy nonselective gray	glossy nonselective white	glossy selective black	glossy selective gray	matte selective black	matte selective gray
laboratory reflectance	0.040	0.200	0.900	0.499	0.573	0.499	0.573
reference reflectance	0.055	0.213	0.902	0.507	0.580	0.499	0.573
daily reflectance	0.082	0.235	0.904	0.541	0.609	0.518	0.589
daily gain (kWh/m²)	516	430	53.8	258	220	271	231
underestimation of reflectance	-0.008 to 0.227	-0.006 to 0.189	-0.001 to 0.024	-0.021 to 0.295	-0.016 to 0.240	-0.042 to 0.296	-0.034 to 0.241
underestimation of daily reflectance	0.027	0.023	0.003	0.034	0.028	0.020	0.016
overestimation of gain (W/m²)	-5.2 to 59.0	-4.4 to 49.2	-0.5 to 6.2	-2.5 to 67.4	-1.9 to 54.8	-5.2 to 69.1	-4.3 to 56.3
overestimation of daily gain (kWh/m²)	15.4	12.9	1.61	19.3	16	11.1	9.01
fractional overestimation of daily gain (%)	3.0	3.0	3.0	7.5	7.3	4.1	3.9

(a–ii) March, west							
	glossy nonselective black	glossy nonselective gray	glossy nonselective white	glossy selective black	glossy selective gray	matte selective black	matte selective gray
laboratory reflectance	0.040	0.200	0.900	0.499	0.573	0.499	0.573
reference reflectance	0.055	0.213	0.902	0.507	0.580	0.499	0.573
daily reflectance	0.082	0.235	0.904	0.541	0.609	0.519	0.590
daily gain (kWh/m²)	517	431	53.9	259	221	271	231
underestimation of reflectance	-0.008 to 0.227	-0.006 to 0.189	-0.001 to 0.024	-0.021 to 0.296	-0.016 to 0.241	-0.042 to 0.297	-0.034 to 0.241
underestimation of daily reflectance	0.027	0.023	0.003	0.034	0.028	0.020	0.016
overestimation of gain (W/m²)	-5.2 to 59.1	-4.4 to 49.2	-0.5 to 6.2	-2.5 to 67.4	-1.9 to 54.8	-5.2 to 69.2	-4.3 to 56.3
overestimation of daily gain (kWh/m²)	15.4	12.8	1.61	19.3	16	11.1	9.05
fractional overestimation of daily gain (%)	3.0	3.0	3.0	7.5	7.3	4.1	3.9

(a–iii) March, south							
	glossy nonselective black	glossy nonselective gray	glossy nonselective white	glossy selective black	glossy selective gray	matte selective black	matte selective gray
laboratory reflectance	0.040	0.200	0.900	0.499	0.573	0.499	0.573
reference reflectance	0.055	0.213	0.902	0.507	0.580	0.499	0.573
daily reflectance	0.110	0.258	0.907	0.533	0.602	0.498	0.573
daily gain (kWh/m²)	658	549	68.6	346	294	371	316
underestimation of reflectance	0.016 to 0.295	0.014 to 0.246	0.002 to 0.031	0.000 to 0.157	0.001 to 0.133	-0.008 to 0.099	-0.007 to 0.081
underestimation of daily reflectance	0.055	0.046	0.006	0.026	0.022	-0.001	-0.001
overestimation of gain (W/m²)	0.4 to 40.4	0.4 to 33.7	0.0 to 4.2	0.3 to 23.4	0.5 to 19.8	-5.8 to 4.9	-4.8 to 4.0
overestimation of daily gain (kWh/m²)	40.7	33.9	4.24	19.2	16.4	-0.584	-0.475
fractional overestimation of daily gain (%)	6.2	6.2	6.2	5.5	5.6	-0.2	-0.2

(a–iv) March, north							
	glossy nonselective black	glossy nonselective gray	glossy nonselective white	glossy selective black	glossy selective gray	matte selective black	matte selective gray
laboratory reflectance	0.040	0.200	0.900	0.499	0.573	0.499	0.573
reference reflectance	0.055	0.213	0.902	0.507	0.580	0.499	0.573
daily reflectance	0.092	0.243	0.905	0.482	0.560	0.452	0.535
daily gain (kWh/m²)	153	128	16	87.4	74.1	92.4	78.3
underestimation of reflectance	0.037 to 0.088	0.031 to 0.073	0.004 to 0.009	-0.056 to 0.142	-0.045 to 0.117	-0.079 to 0.123	-0.064 to 0.100
underestimation of daily reflectance	0.037	0.031	0.004	-0.025	-0.020	-0.047	-0.038
overestimation of gain (W/m²)	0.5 to 5.1	0.4 to 4.2	0.1 to 0.5	-3.3 to 1.8	-2.6 to 1.5	-5.3 to 1.6	-4.3 to 1.3
overestimation of daily gain (kWh/m²)	6.22	5.18	0.648	-4.25	-3.34	-7.88	-6.41
fractional overestimation of daily gain (%)	4.1	4.1	4.1	-4.9	-4.5	-8.5	-8.2

(b–i) June, east							
	glossy nonselective black	glossy nonselective gray	glossy nonselective white	glossy selective black	glossy selective gray	matte selective black	matte selective gray
laboratory reflectance	0.040	0.200	0.900	0.499	0.573	0.499	0.573
reference reflectance	0.055	0.213	0.902	0.507	0.580	0.499	0.573
daily reflectance	0.080	0.233	0.904	0.533	0.602	0.511	0.584
daily gain (kWh/m²)	674	562	70.3	343	292	358	305
underestimation of reflectance	-0.007 to 0.217	-0.006 to 0.181	-0.001 to 0.023	-0.026 to 0.289	-0.020 to 0.236	-0.047 to 0.289	-0.038 to 0.236
underestimation of daily reflectance	0.025	0.021	0.003	0.026	0.022	0.012	0.010
overestimation of gain (W/m²)	-5.2 to 62.0	-4.3 to 51.7	-0.5 to 6.5	-2.3 to 61.2	-1.8 to 49.8	-7.3 to 62.7	-6.0 to 51.0
overestimation of daily gain (kWh/m²)	18.4	15.3	1.92	19	15.8	9.07	7.38
fractional overestimation of daily gain (%)	2.7	2.7	2.7	5.5	5.4	2.5	2.4

(b–ii) June, west							
	glossy nonselective black	glossy nonselective gray	glossy nonselective white	glossy selective black	glossy selective gray	matte selective black	matte selective gray
laboratory reflectance	0.040	0.200	0.900	0.499	0.573	0.499	0.573
reference reflectance	0.055	0.213	0.902	0.507	0.580	0.499	0.573
daily reflectance	0.080	0.233	0.904	0.533	0.602	0.511	0.584
daily gain (kWh/m²)	675	562	70.3	343	292	358	305
underestimation of reflectance	-0.007 to 0.217	-0.006 to 0.181	-0.001 to 0.023	-0.025 to 0.291	-0.020 to 0.237	-0.047 to 0.291	-0.038 to 0.237
underestimation of daily reflectance	0.025	0.021	0.003	0.026	0.022	0.012	0.010
overestimation of gain (W/m²)	-5.2 to 62.0	-4.3 to 51.7	-0.5 to 6.5	-2.3 to 61.4	-1.8 to 49.9	-7.3 to 62.9	-6.0 to 51.2
overestimation of daily gain (kWh/m²)	18.4	15.3	1.92	19	15.8	9.11	7.42
fractional overestimation of daily gain (%)	2.7	2.7	2.7	5.6	5.4	2.5	2.4

(b–iii) June, south							
	glossy nonselective black	glossy nonselective gray	glossy nonselective white	glossy selective black	glossy selective gray	matte selective black	matte selective gray
laboratory reflectance	0.040	0.200	0.900	0.499	0.573	0.499	0.573
reference reflectance	0.055	0.213	0.902	0.507	0.580	0.499	0.573
daily reflectance	0.207	0.339	0.917	0.561	0.627	0.471	0.551
daily gain (kWh/m²)	305	254	31.7	169	143	203	173
underestimation of reflectance	0.037 to 0.228	0.031 to 0.190	0.004 to 0.024	-0.050 to 0.098	-0.040 to 0.084	-0.072 to 0.055	-0.059 to 0.045
underestimation of daily reflectance	0.152	0.127	0.016	0.054	0.047	-0.028	-0.022
overestimation of gain (W/m²)	0.3 to 60.9	0.2 to 50.8	0.0 to 6.3	-3.6 to 26.7	-2.8 to 22.9	-7.2 to 0.4	-5.9 to 0.3
overestimation of daily gain (kWh/m²)	58.6	48.8	6.1	20.7	18	-10.6	-8.61
fractional overestimation of daily gain (%)	19.2	19.2	19.2	12.3	12.6	-5.2	-5.0

(b–iv) June, north							
	glossy nonselective black	glossy nonselective gray	glossy nonselective white	glossy selective black	glossy selective gray	matte selective black	matte selective gray
laboratory reflectance	0.040	0.200	0.900	0.499	0.573	0.499	0.573
reference reflectance	0.055	0.213	0.902	0.507	0.580	0.499	0.573
daily reflectance	0.157	0.297	0.912	0.565	0.629	0.507	0.580
daily gain (kWh/m²)	304	254	31.7	157	134	178	151
underestimation of reflectance	0.035 to 0.249	0.029 to 0.207	0.004 to 0.026	-0.025 to 0.276	-0.020 to 0.225	-0.046 to 0.272	-0.038 to 0.221
underestimation of daily reflectance	0.102	0.085	0.011	0.058	0.049	0.009	0.007
overestimation of gain (W/m²)	1.6 to 49.2	1.3 to 41.0	0.2 to 5.1	-3.1 to 31.7	-2.4 to 26.0	-5.7 to 29.0	-4.6 to 23.6
overestimation of daily gain (kWh/m²)	36.6	30.5	3.82	20.9	17.7	3.08	2.51
fractional overestimation of daily gain (%)	12.0	12.0	12.0	13.3	13.3	1.7	1.7

(c–i) September, east							
	glossy nonselective black	glossy nonselective gray	glossy nonselective white	glossy selective black	glossy selective gray	matte selective black	matte selective gray
laboratory reflectance	0.040	0.200	0.900	0.499	0.573	0.499	0.573
reference reflectance	0.055	0.213	0.902	0.507	0.580	0.499	0.573
daily reflectance	0.082	0.235	0.904	0.541	0.609	0.519	0.590
daily gain (kWh/m²)	515	429	53.6	257	219	270	230
underestimation of reflectance	-0.008 to 0.227	-0.006 to 0.189	-0.001 to 0.024	-0.021 to 0.298	-0.017 to 0.242	-0.042 to 0.298	-0.035 to 0.243
underestimation of daily reflectance	0.027	0.023	0.003	0.035	0.029	0.020	0.016
overestimation of gain (W/m²)	-5.2 to 59.0	-4.4 to 49.2	-0.5 to 6.1	-2.5 to 67.3	-1.9 to 54.7	-5.2 to 69.0	-4.3 to 56.2
overestimation of daily gain (kWh/m²)	15.4	12.8	1.6	19.4	16.1	11.2	9.09
fractional overestimation of daily gain (%)	3.0	3.0	3.0	7.5	7.3	4.1	3.9

(c–ii) September, west							
	glossy nonselective black	glossy nonselective gray	glossy nonselective white	glossy selective black	glossy selective gray	matte selective black	matte selective gray
laboratory reflectance	0.040	0.200	0.900	0.499	0.573	0.499	0.573
reference reflectance	0.055	0.213	0.902	0.507	0.580	0.499	0.573
daily reflectance	0.083	0.235	0.904	0.541	0.609	0.519	0.590
daily gain (kWh/m²)	513	428	53.5	257	219	269	230
underestimation of reflectance	-0.008 to 0.227	-0.006 to 0.189	-0.001 to 0.024	-0.021 to 0.298	-0.016 to 0.242	-0.042 to 0.298	-0.035 to 0.242
underestimation of daily reflectance	0.028	0.023	0.003	0.035	0.029	0.020	0.016
overestimation of gain (W/m²)	-5.2 to 59.0	-4.3 to 49.2	-0.5 to 6.1	-2.5 to 67.3	-1.9 to 54.7	-5.2 to 69.0	-4.3 to 56.2
overestimation of daily gain (kWh/m²)	15.4	12.8	1.61	19.3	16	11.1	9.06
fractional overestimation of daily gain (%)	3.0	3.0	3.0	7.5	7.3	4.1	3.9

(c–iii) September, south							
	glossy nonselective black	glossy nonselective gray	glossy nonselective white	glossy selective black	glossy selective gray	matte selective black	matte selective gray
laboratory reflectance	0.040	0.200	0.900	0.499	0.573	0.499	0.573
reference reflectance	0.055	0.213	0.902	0.507	0.580	0.499	0.573
daily reflectance	0.109	0.257	0.907	0.533	0.602	0.498	0.573
daily gain (kWh/m²)	663	552	69	348	296	373	317
underestimation of reflectance	0.016 to 0.295	0.013 to 0.246	0.002 to 0.031	0.000 to 0.160	0.001 to 0.136	-0.008 to 0.112	-0.007 to 0.091
underestimation of daily reflectance	0.054	0.045	0.006	0.026	0.022	-0.000	-0.000
overestimation of gain (W/m²)	0.4 to 39.9	0.3 to 33.3	0.0 to 4.2	0.2 to 23.5	0.4 to 19.9	-5.7 to 5.3	-4.7 to 4.3
overestimation of daily gain (kWh/m²)	40	33.4	4.17	19.1	16.3	-0.228	-0.186
fractional overestimation of daily gain (%)	6.0	6.0	6.0	5.5	5.5	-0.1	-0.1

(c–iv) September, north							
	glossy nonselective black	glossy nonselective gray	glossy nonselective white	glossy selective black	glossy selective gray	matte selective black	matte selective gray
laboratory reflectance	0.040	0.200	0.900	0.499	0.573	0.499	0.573
reference reflectance	0.055	0.213	0.902	0.507	0.580	0.499	0.573
daily reflectance	0.092	0.243	0.905	0.482	0.560	0.452	0.535
daily gain (kWh/m²)	152	127	15.9	87	73.8	92	78
underestimation of reflectance	0.037 to 0.073	0.031 to 0.061	0.004 to 0.008	-0.055 to 0.145	-0.044 to 0.119	-0.079 to 0.129	-0.064 to 0.105
underestimation of daily reflectance	0.037	0.031	0.004	-0.025	-0.020	-0.047	-0.038
overestimation of gain (W/m²)	0.5 to 5.1	0.4 to 4.2	0.0 to 0.5	-3.3 to 1.7	-2.6 to 1.4	-5.3 to 1.5	-4.3 to 1.3
overestimation of daily gain (kWh/m²)	6.18	5.15	0.644	-4.23	-3.33	-7.84	-6.38
fractional overestimation of daily gain (%)	4.1	4.1	4.1	-4.9	-4.5	-8.5	-8.2

(d–i) December, east							
	glossy nonselective black	glossy nonselective gray	glossy nonselective white	glossy selective black	glossy selective gray	matte selective black	matte selective gray
laboratory reflectance	0.040	0.200	0.900	0.499	0.573	0.499	0.573
reference reflectance	0.055	0.213	0.902	0.507	0.580	0.499	0.573
daily reflectance	0.103	0.253	0.907	0.569	0.632	0.537	0.604
daily gain (kWh/m²)	261	217	27.1	125	107	135	115
underestimation of reflectance	-0.004 to 0.253	-0.003 to 0.211	-0.000 to 0.026	-0.039 to 0.288	-0.031 to 0.234	-0.061 to 0.288	-0.050 to 0.234
underestimation of daily reflectance	0.048	0.040	0.005	0.062	0.051	0.038	0.031
overestimation of gain (W/m²)	-1.2 to 50.1	-1.0 to 41.7	-0.1 to 5.2	-3.7 to 55.7	-3.0 to 45.3	-5.9 to 56.6	-4.8 to 46.1
overestimation of daily gain (kWh/m²)	14.1	11.7	1.46	18	15	11	8.95
fractional overestimation of daily gain (%)	5.4	5.4	5.4	14.4	14.0	8.2	7.8

(d–ii) December, west							
	glossy nonselective black	glossy nonselective gray	glossy nonselective white	glossy selective black	glossy selective gray	matte selective black	matte selective gray
laboratory reflectance	0.040	0.200	0.900	0.499	0.573	0.499	0.573
reference reflectance	0.055	0.213	0.902	0.507	0.580	0.499	0.573
daily reflectance	0.103	0.253	0.907	0.569	0.632	0.536	0.604
daily gain (kWh/m²)	260	217	27.1	125	107	135	115
underestimation of reflectance	-0.004 to 0.253	-0.003 to 0.211	-0.000 to 0.026	-0.038 to 0.285	-0.031 to 0.232	-0.061 to 0.286	-0.049 to 0.233
underestimation of daily reflectance	0.048	0.040	0.005	0.062	0.051	0.038	0.031
overestimation of gain (W/m²)	-1.2 to 50.1	-1.0 to 41.8	-0.1 to 5.2	-3.7 to 55.6	-3.0 to 45.3	-5.9 to 56.6	-4.8 to 46.1
overestimation of daily gain (kWh/m²)	14.1	11.7	1.46	18	14.9	10.9	8.87
fractional overestimation of daily gain (%)	5.4	5.4	5.4	14.3	13.9	8.1	7.7

(d–iii) December, south							
	glossy nonselective black	glossy nonselective gray	glossy nonselective white	glossy selective black	glossy selective gray	matte selective black	matte selective gray
laboratory reflectance	0.040	0.200	0.900	0.499	0.573	0.499	0.573
reference reflectance	0.055	0.213	0.902	0.507	0.580	0.499	0.573
daily reflectance	0.054	0.212	0.901	0.547	0.613	0.540	0.607
daily gain (kWh/m²)	754	629	78.6	361	309	367	313
underestimation of reflectance	-0.006 to 0.036	-0.005 to 0.030	-0.001 to 0.004	0.013 to 0.272	0.010 to 0.222	0.016 to 0.267	0.013 to 0.217
underestimation of daily reflectance	-0.001	-0.001	-0.000	0.040	0.033	0.041	0.034
overestimation of gain (W/m²)	-4.8 to 4.6	-4.0 to 3.8	-0.5 to 0.5	10.5 to 41.0	8.4 to 33.5	13.1 to 39.8	10.6 to 32.4
overestimation of daily gain (kWh/m²)	-0.829	-0.691	-0.0864	32.1	26.1	33.1	26.9
fractional overestimation of daily gain (%)	-0.1	-0.1	-0.1	8.9	8.5	9.0	8.6

(d–iv) December, north							
	glossy nonselective black	glossy nonselective gray	glossy nonselective white	glossy selective black	glossy selective gray	matte selective black	matte selective gray
laboratory reflectance	0.040	0.200	0.900	0.499	0.573	0.499	0.573
reference reflectance	0.055	0.213	0.902	0.507	0.580	0.499	0.573
daily reflectance	0.092	0.243	0.905	0.483	0.561	0.453	0.536
daily gain (kWh/m²)	89.6	74.7	9.34	51.1	43.3	54	45.8
underestimation of reflectance	0.037 to 0.037	0.031 to 0.031	0.004 to 0.004	-0.042 to 0.043	-0.034 to 0.036	-0.065 to 0.025	-0.053 to 0.021
underestimation of daily reflectance	0.037	0.031	0.004	-0.024	-0.019	-0.046	-0.037
overestimation of gain (W/m²)	0.3 to 3.9	0.3 to 3.2	0.0 to 0.4	-2.1 to 0.4	-1.6 to 0.3	-4.2 to 0.2	-3.4 to 0.2
overestimation of daily gain (kWh/m²)	3.63	3.02	0.378	-2.39	-1.87	-4.5	-3.67
fractional overestimation of daily gain (%)	4.0	4.0	4.0	-4.7	-4.3	-8.3	-8.0

Table 3. Rises in laboratory, reference, and daily solar reflectances, and overestimations of rises in solar reflectance when substituting laboratory or reference solar reflectance for daily solar reflectance, by wall direction (E, W, S, N) and season (summer = Jun/Jul/Aug, winter = Dec/Jan/Feb), at latitude 37°N. Values are shown for upgrading a *glossy* surface (a) from nonselective black to nonselective white, (b) from nonselective gray to nonselective white, (c) from nonselective black to selective black, and (d) from nonselective gray to selective gray; and for upgrading a *matte* surface (e) from nonselective black to selective black, and (f) from nonselective gray to selective gray.

(a) glossy: nonselective black to nonselective white								
	E/summer	E/winter	W/summer	W/winter	S/summer	S/winter	N/summer	N/winter
rise in laboratory reflectance	0.860	0.860	0.860	0.860	0.860	0.860	0.860	0.860
rise in reference reflectance	0.847	0.847	0.847	0.847	0.847	0.847	0.847	0.847
rise in daily reflectance	0.824	0.809	0.824	0.809	0.728	0.841	0.764	0.814
refl. rise overestimation using lab reflectance (%)	4.3	6.3	4.3	6.3	18.2	2.3	12.5	5.7
refl. rise overestimation using ref. reflectance (%)	2.7	4.6	2.7	4.6	16.3	0.7	10.8	4.0

(b) glossy: nonselective gray to nonselective white								
	E/summer	E/winter	W/summer	W/winter	S/summer	S/winter	N/summer	N/winter
rise in laboratory reflectance	0.700	0.700	0.700	0.700	0.700	0.700	0.700	0.700
rise in reference reflectance	0.689	0.689	0.689	0.689	0.689	0.689	0.689	0.689
rise in daily reflectance	0.671	0.659	0.671	0.659	0.592	0.684	0.622	0.662
refl. rise overestimation using lab reflectance (%)	4.3	6.3	4.3	6.3	18.2	2.3	12.5	5.7
refl. rise overestimation using ref. reflectance (%)	2.7	4.6	2.7	4.6	16.3	0.7	10.8	4.0

(c) glossy: nonselective black to selective black								
	E/summer	E/winter	W/summer	W/winter	S/summer	S/winter	N/summer	N/winter
rise in laboratory reflectance	0.459	0.459	0.459	0.459	0.459	0.459	0.459	0.459
rise in reference reflectance	0.452	0.452	0.452	0.452	0.452	0.452	0.452	0.452
rise in daily reflectance	0.454	0.464	0.454	0.464	0.367	0.478	0.399	0.390
refl. rise overestimation using lab reflectance (%)	1.0	-1.1	1.1	-1.1	25.0	-4.0	15.0	17.6
refl. rise overestimation using ref. reflectance (%)	-0.5	-2.6	-0.5	-2.6	23.1	-5.5	13.2	15.8

(d) glossy: nonselective gray to selective gray								
	E/summer	E/winter	W/summer	W/winter	S/summer	S/winter	N/summer	N/winter
rise in laboratory reflectance	0.373	0.373	0.373	0.373	0.373	0.373	0.373	0.373
rise in reference reflectance	0.368	0.368	0.368	0.368	0.368	0.368	0.368	0.368
rise in daily reflectance	0.370	0.378	0.370	0.378	0.299	0.389	0.325	0.318
refl. rise overestimation using lab reflectance (%)	1.0	-1.1	1.1	-1.1	25.0	-4.0	15.0	17.6
refl. rise overestimation using ref. reflectance (%)	-0.5	-2.6	-0.5	-2.6	23.1	-5.5	13.2	15.8

(e) matte: nonselective black to selective black								
	E/summer	E/winter	W/summer	W/winter	S/summer	S/winter	N/summer	N/winter
rise in laboratory reflectance	0.459	0.459	0.459	0.459	0.459	0.459	0.459	0.459
rise in reference reflectance	0.459	0.459	0.459	0.459	0.459	0.459	0.459	0.459
rise in daily reflectance	0.473	0.491	0.472	0.491	0.436	0.489	0.454	0.413
refl. rise overestimation using lab reflectance (%)	-2.9	-6.6	-2.9	-6.6	5.1	-6.2	1.1	11.2
refl. rise overestimation using ref. reflectance (%)	-2.9	-6.6	-2.9	-6.6	5.1	-6.2	1.1	11.2

(f) matte: nonselective gray to selective gray								
	E/summer	E/winter	W/summer	W/winter	S/summer	S/winter	N/summer	N/winter
rise in laboratory reflectance	0.373	0.373	0.373	0.373	0.373	0.373	0.373	0.373
rise in reference reflectance	0.373	0.373	0.373	0.373	0.373	0.373	0.373	0.373
rise in daily reflectance	0.385	0.400	0.385	0.400	0.355	0.398	0.370	0.336
refl. rise overestimation using lab reflectance (%)	-2.9	-6.6	-2.9	-6.6	5.1	-6.2	1.1	11.2
refl. rise overestimation using ref. reflectance (%)	-2.9	-6.6	-2.9	-6.6	5.1	-6.2	1.1	11.2

Table 4. Specular solar reflectance (specular component of air mass 1 global horizontal solar reflectance) of (1) a diffuse reflectance standard; (2) a specular reflectance standard (mirror); (3) an unbacked glass microscope slide; (4) the glass slide with an opaque black undercoating; (5) the black undercoating; and (6-20) an assortment of wall products. Nominal finish comes from the product label, while LBNL assessment of finish is visual.

#	Description	Color	Coating application	Substrate	Nominal finish	LBNL assessment of finish	Specular solar reflectance
1	Spectralon SRS-99 diffuse reflectance standard	white					0.001
2	Specular reflectance standard	silver					0.888
3	Unbacked glass slide	clear					0.079
4	Glass slide with opaque black paint undercoating, glass side forward	black	field	glass			0.042
5	Glass slide with opaque black paint undercoating, painted side forward	black	field	glass		semigloss	0.004
6	(redacted)	black	factory	metal		semigloss	0.018
7	(redacted)	light gray	factory	metal		semigloss	0.016
8	(redacted)	white	factory	metal		semigloss	0.018
9	(redacted)	dark brown	factory	metal		semigloss	0.023
10	(redacted)	white	factory	metal		semigloss	0.026
11	(redacted)	dark gray-blue	field	wood	semigloss	semigloss	0.020
12	(redacted)	white	field	wood	semigloss	semigloss	0.020
13	(redacted)	light brown	field	fiber cement	semigloss	semigloss	0.005
14	(redacted)	light brown	field	fiber cement	satin	satin	0.004
15	(redacted)	white	field	fiber cement	satin	satin	0.001
16	(redacted)	dark brown	field	wood		matte	0.001
17	(redacted)	light gray-green	field	wood		matte	0.005
18	(redacted)	peach	field	wood		matte	0.006
19	(redacted)	dark gray-green	field	metal		matte	0.000
20	(redacted)	peach	field	metal		matte	0.005

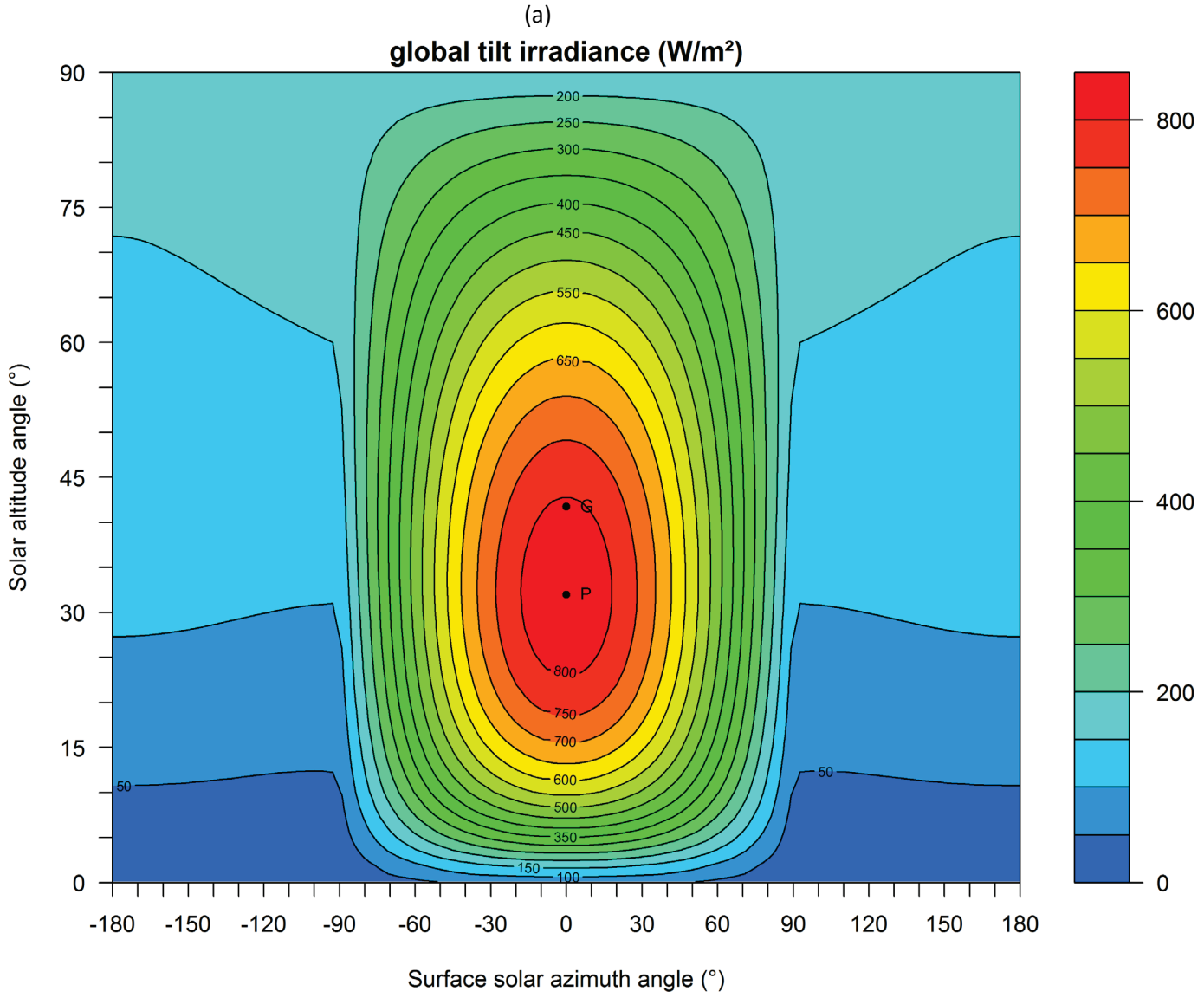

Figure 12. Variations with solar position of a wall's (a) global (beam + diffuse) tilt irradiance; (b) beam tilt irradiance; (c) diffuse tilt irradiance; (d) NIR fraction of global tilt irradiance; and (e) diffuse fraction of global tilt irradiance. Note that surface solar azimuth angle = solar azimuth angle – surface azimuth angle.

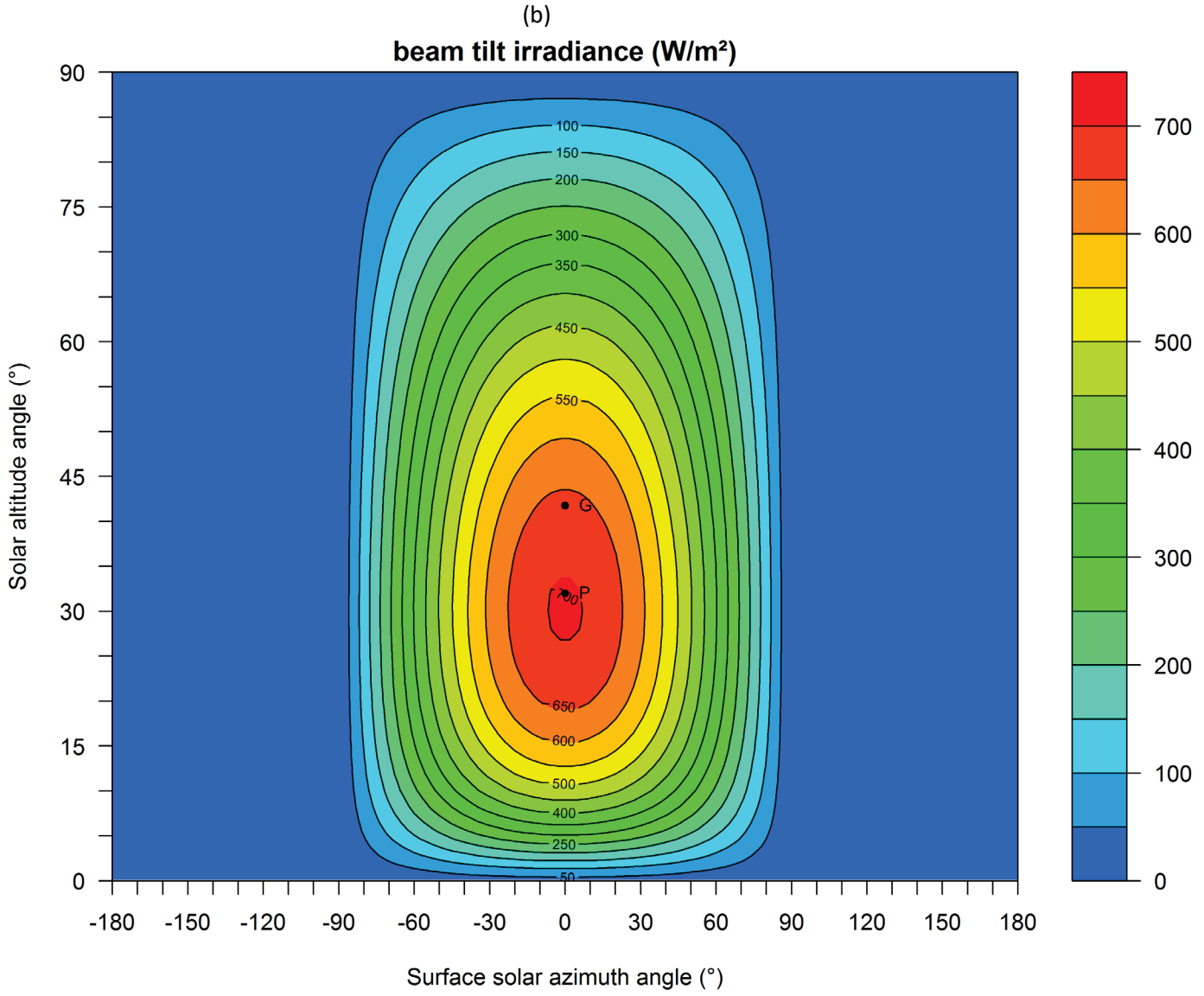

Figure 12 (continued)

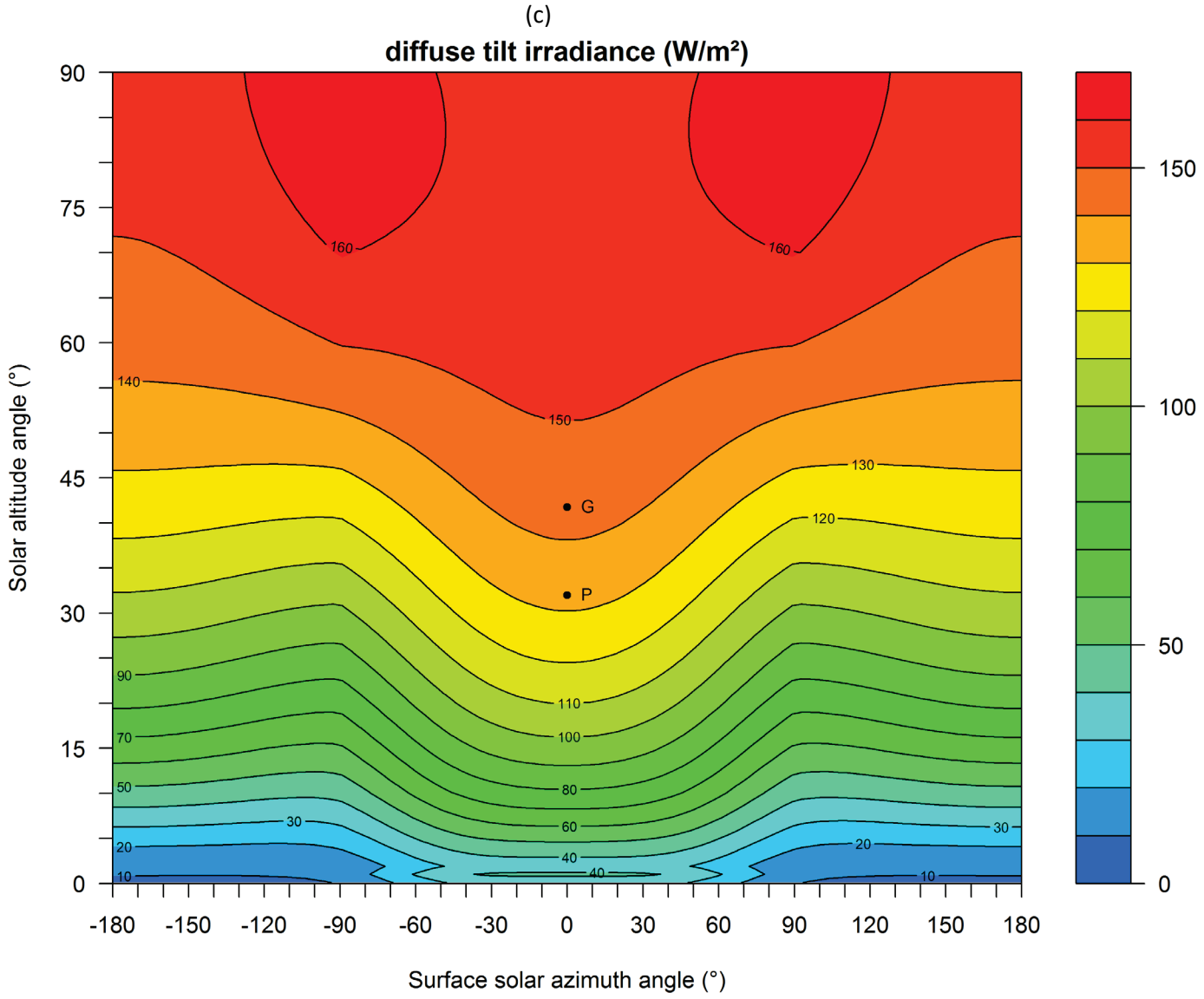

Figure 12 (continued)

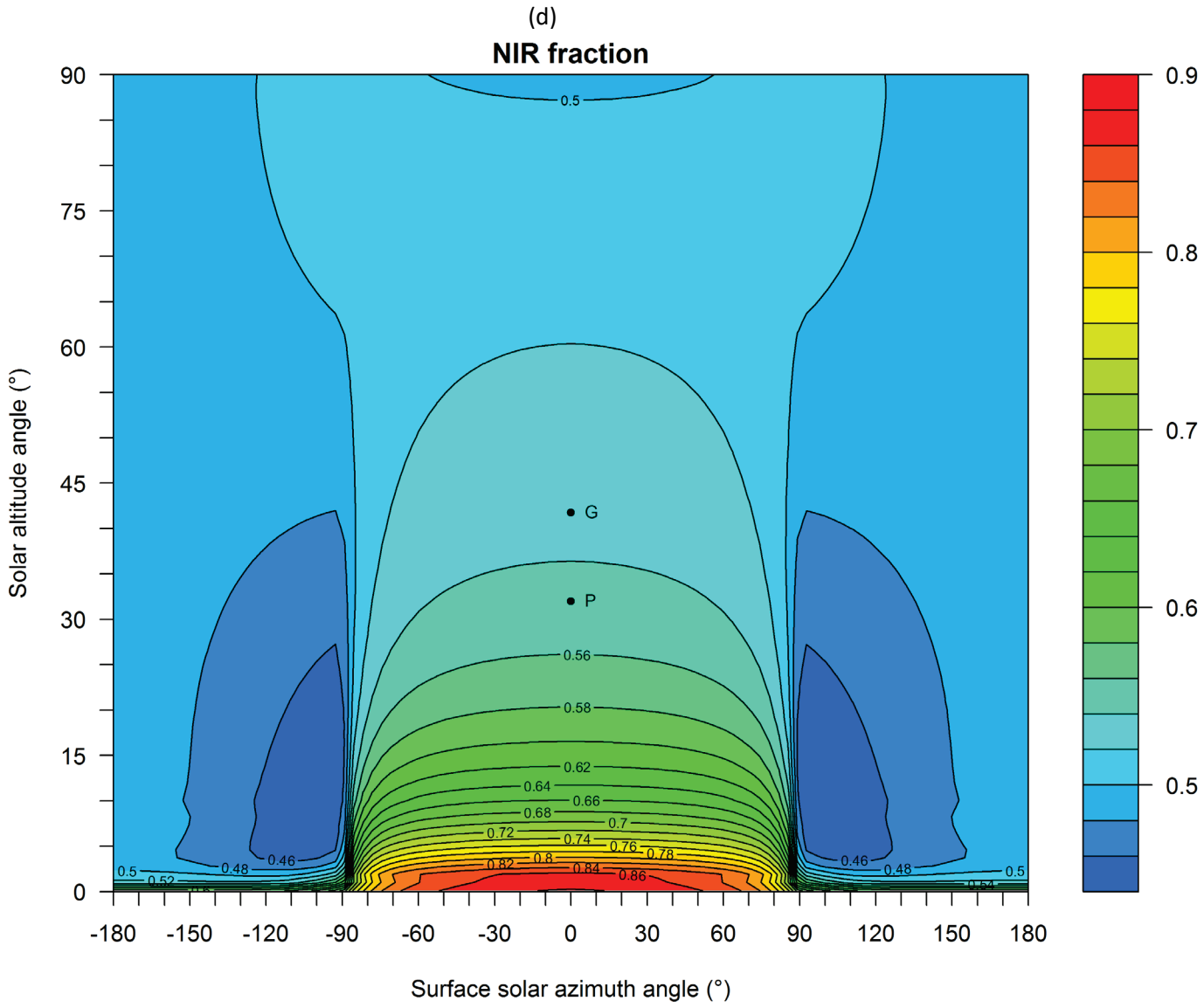

Figure 12 (continued)

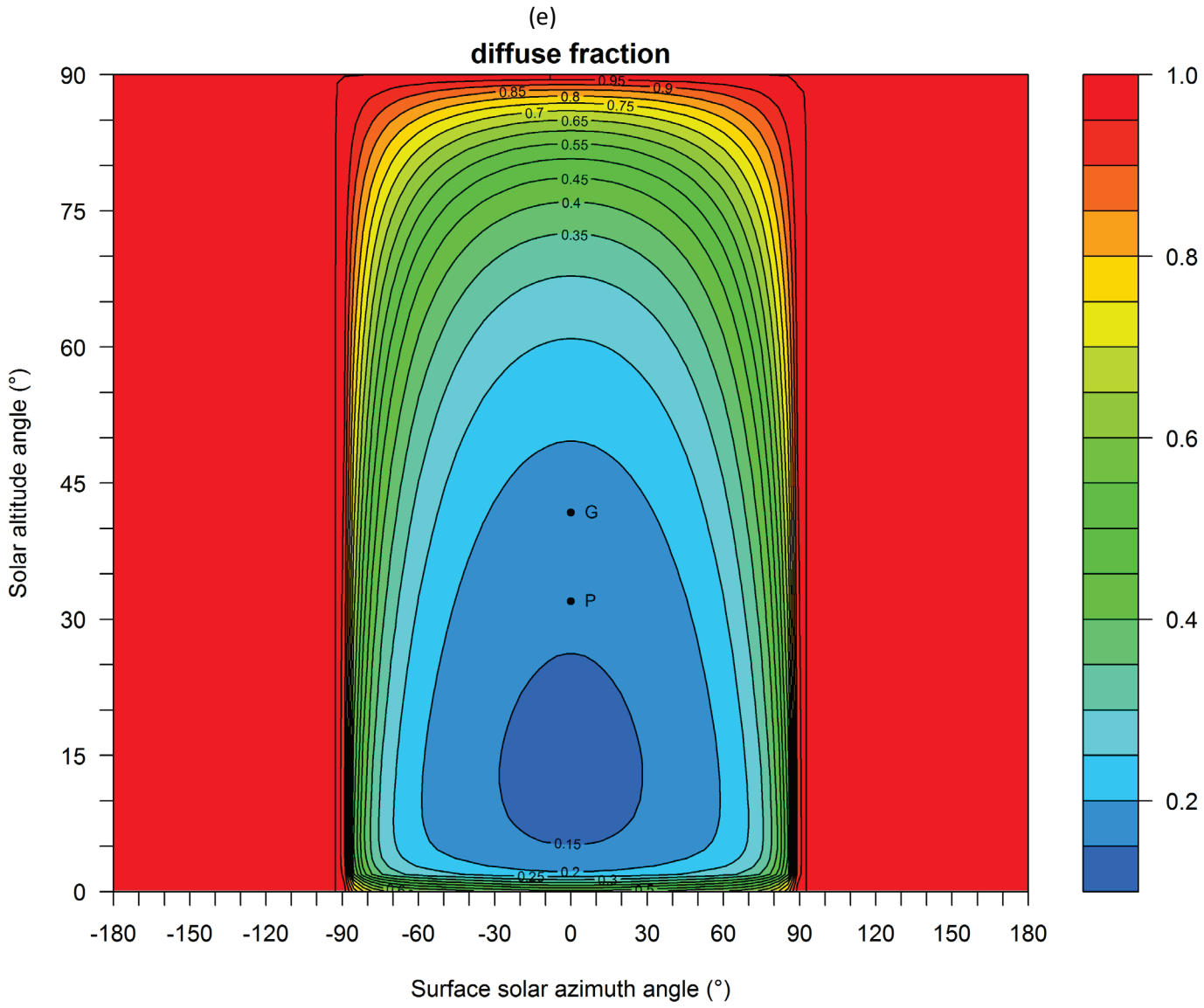

Figure 12 (continued)

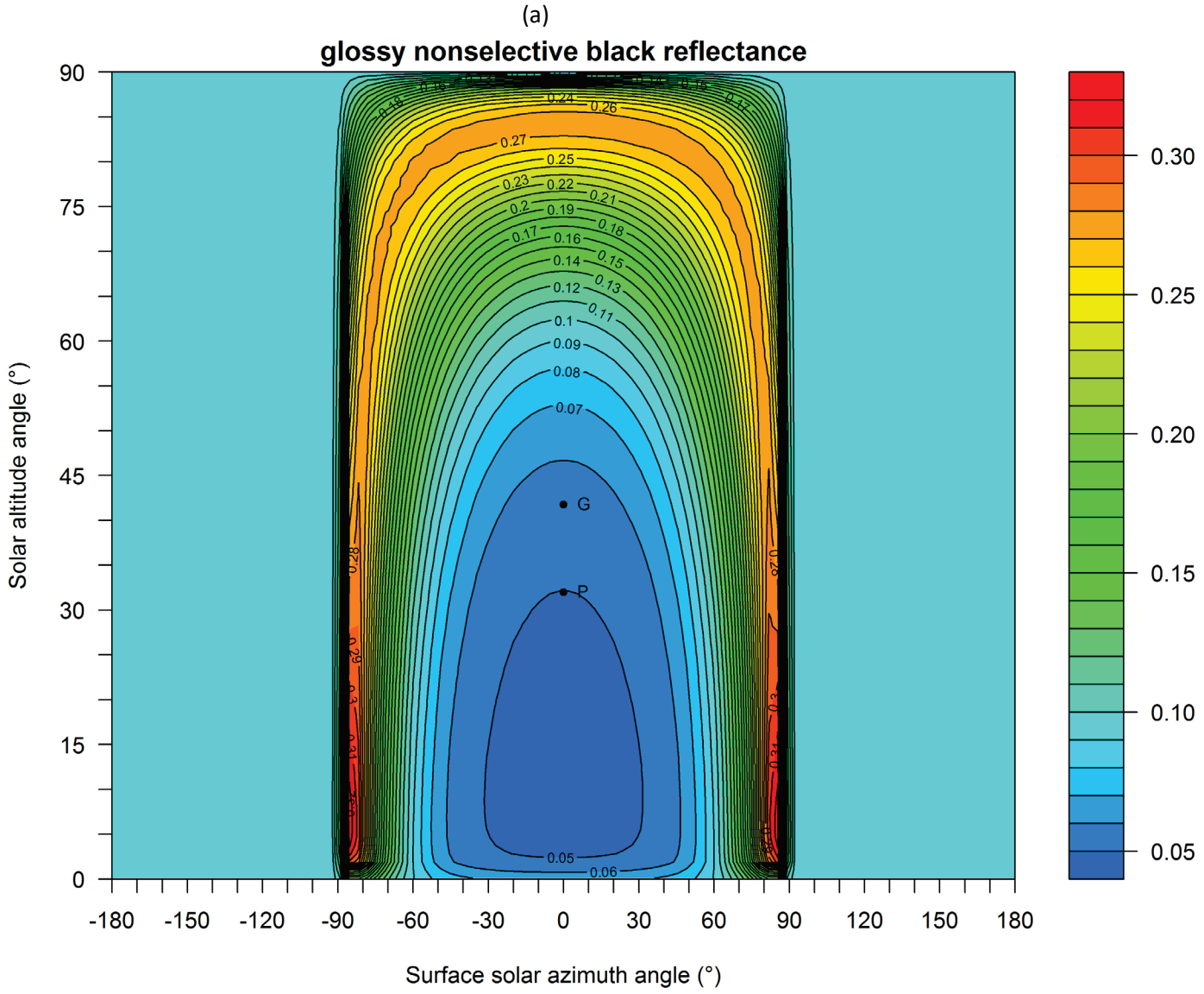

Figure 13. Variations with solar position of the global solar reflectances of seven ideal walls: (a) glossy nonselective black, (b) glossy nonselective gray; (c) glossy nonselective white; (d) glossy selective black; (e) glossy selective gray; (f) matte selective black; and (g) matte selective gray. Note that surface solar azimuth angle = solar azimuth angle – surface azimuth angle.

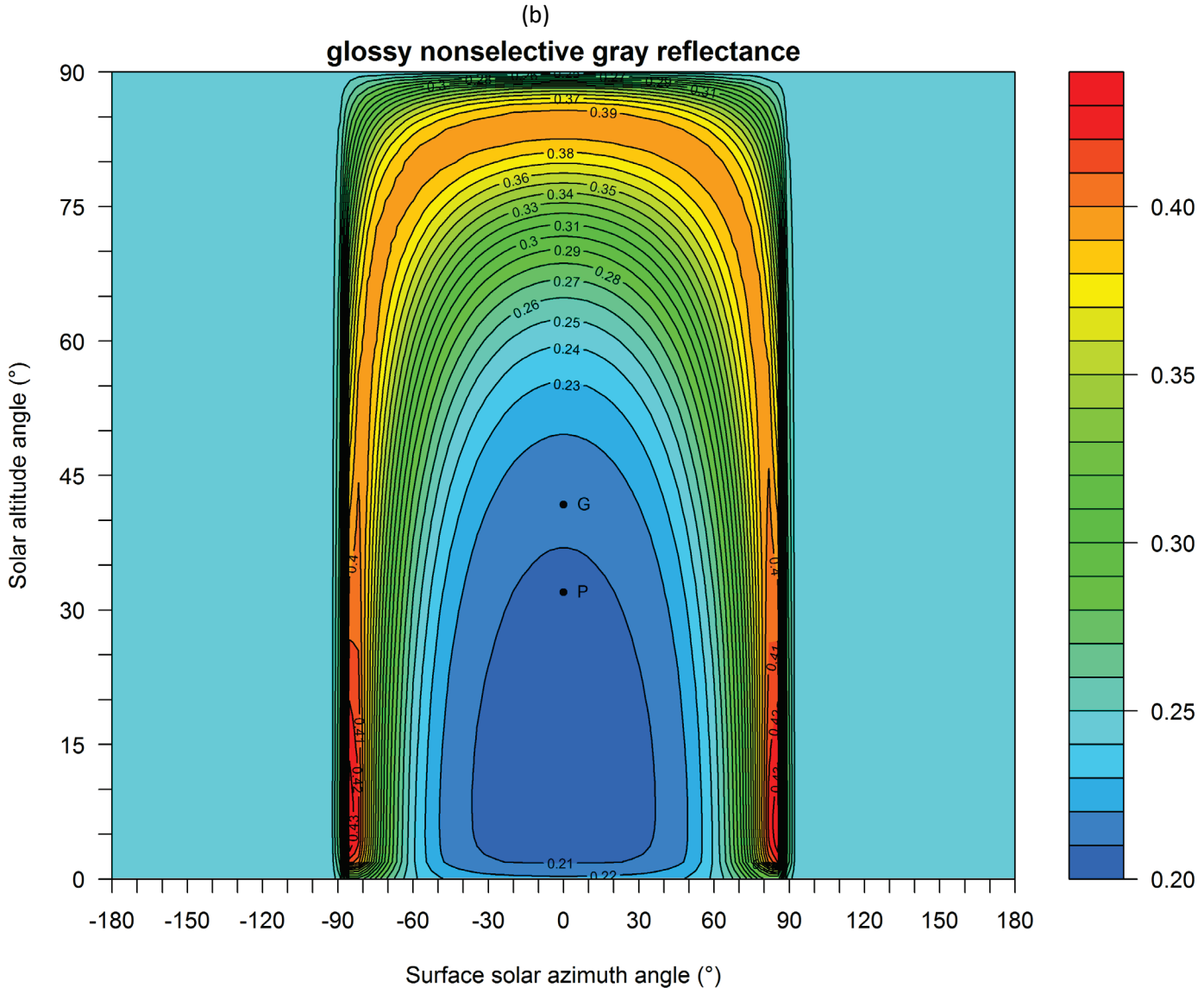

Figure 13 (continued)

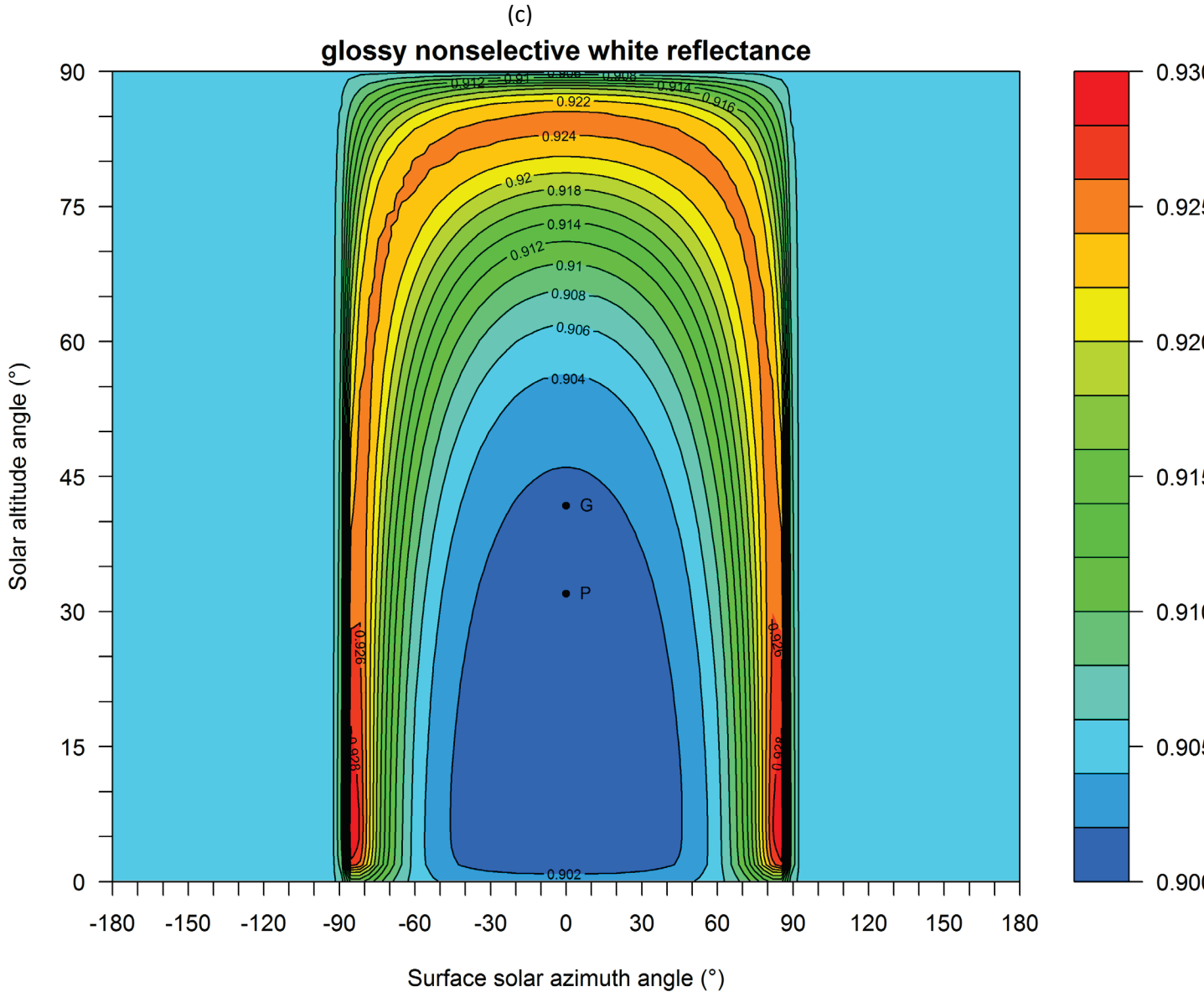

Figure 13 (continued)

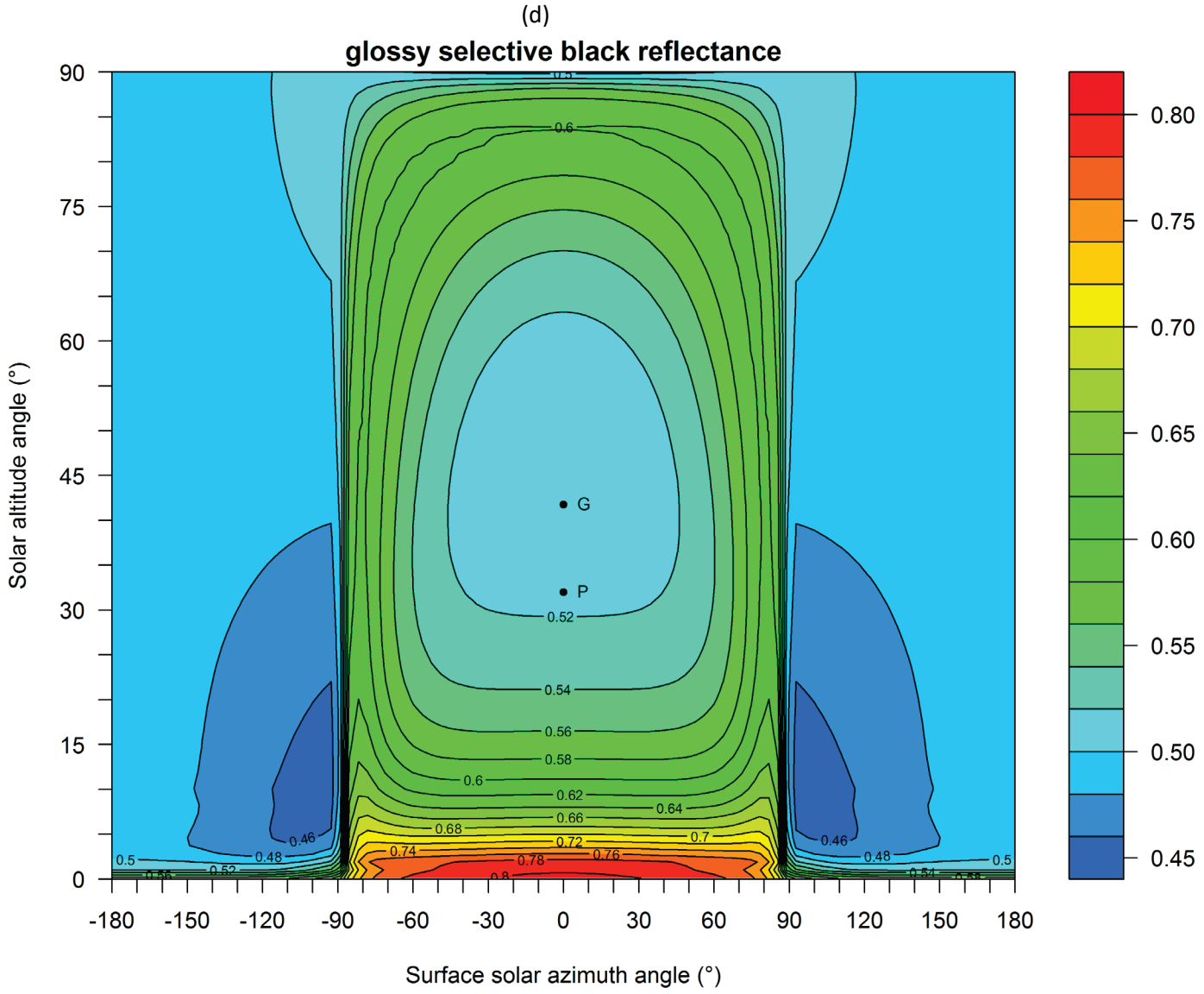

Figure 13 (continued)

(e)

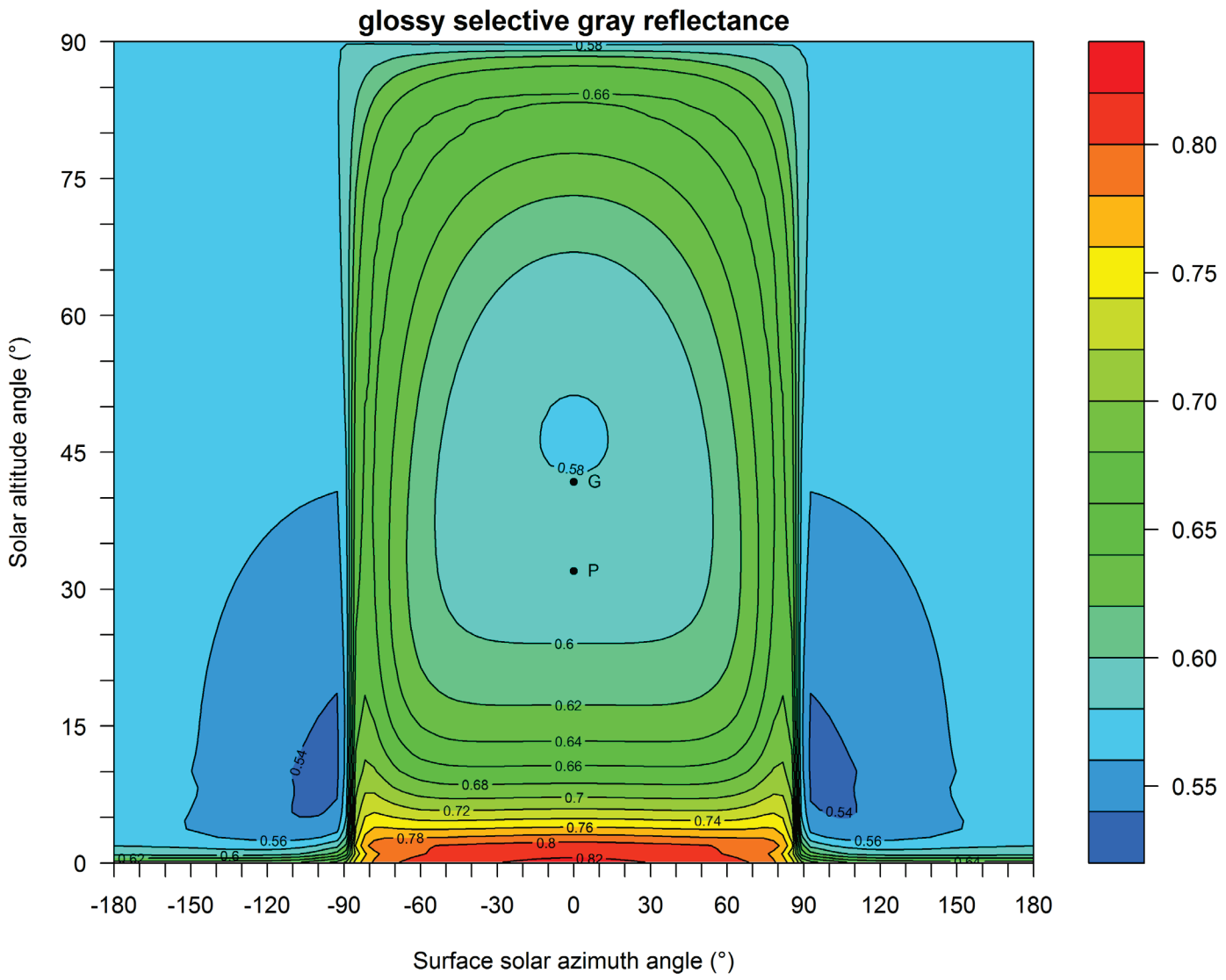

Figure 13 (continued)

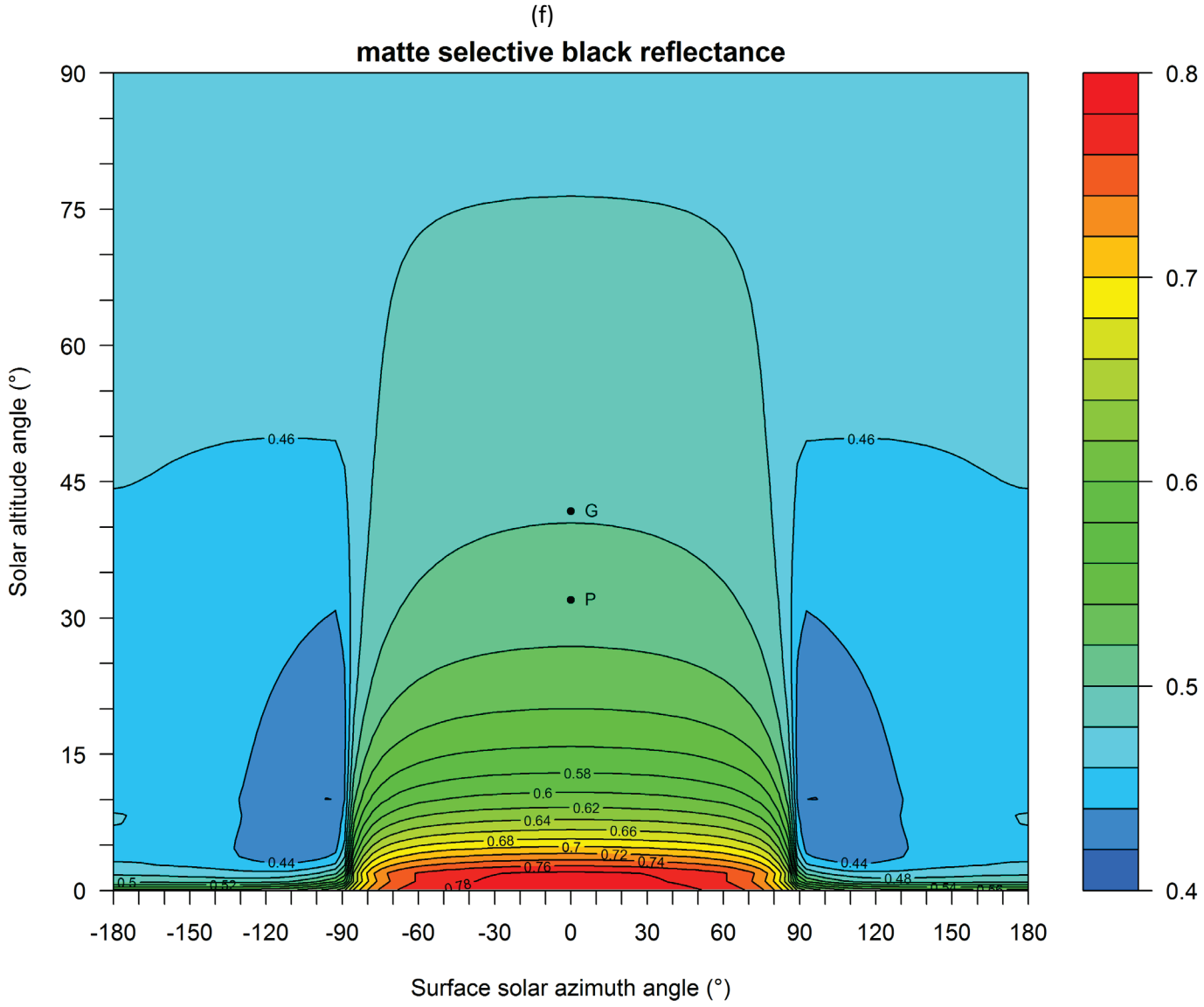

Figure 13 (continued)

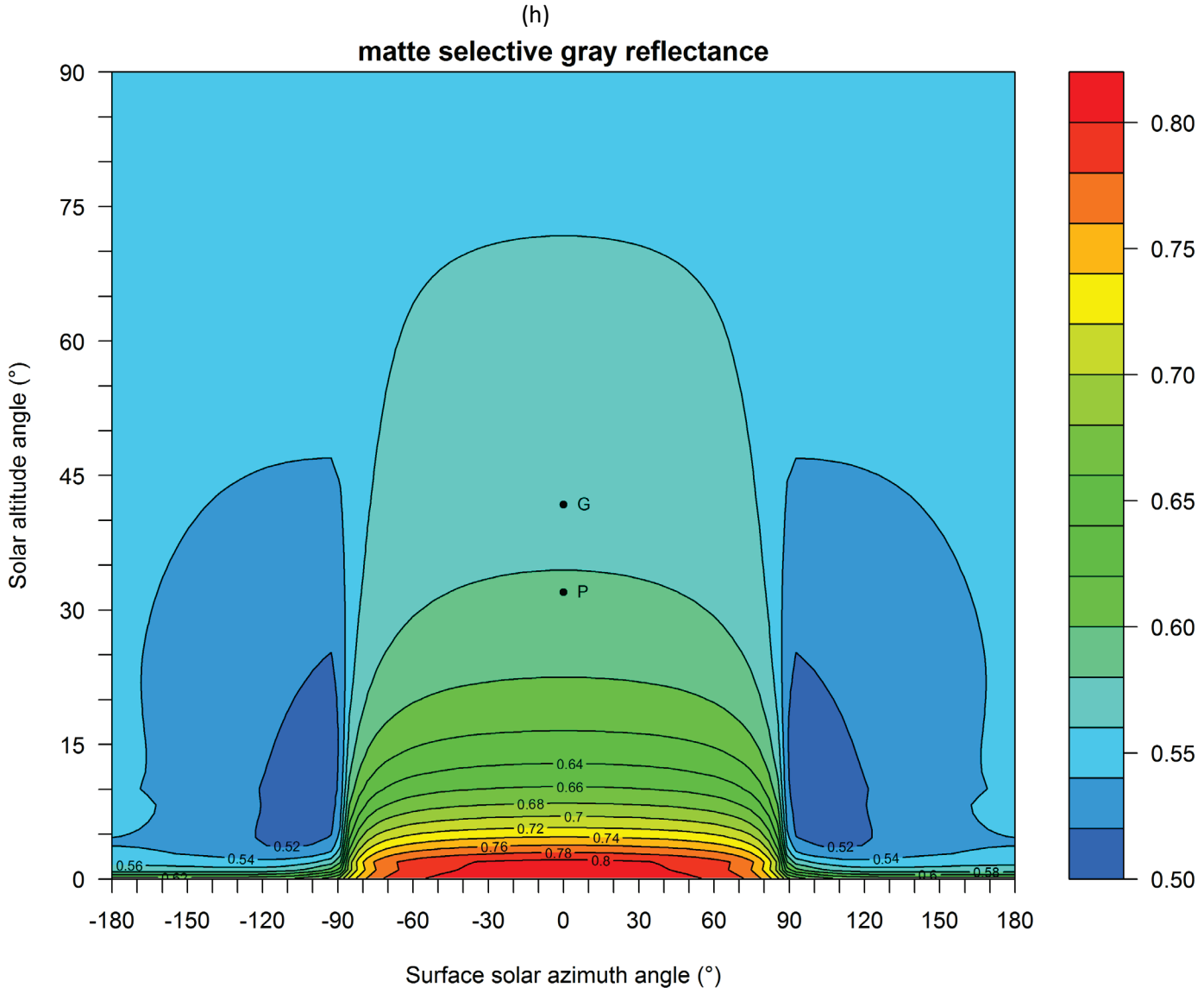

Figure 13 (continued)

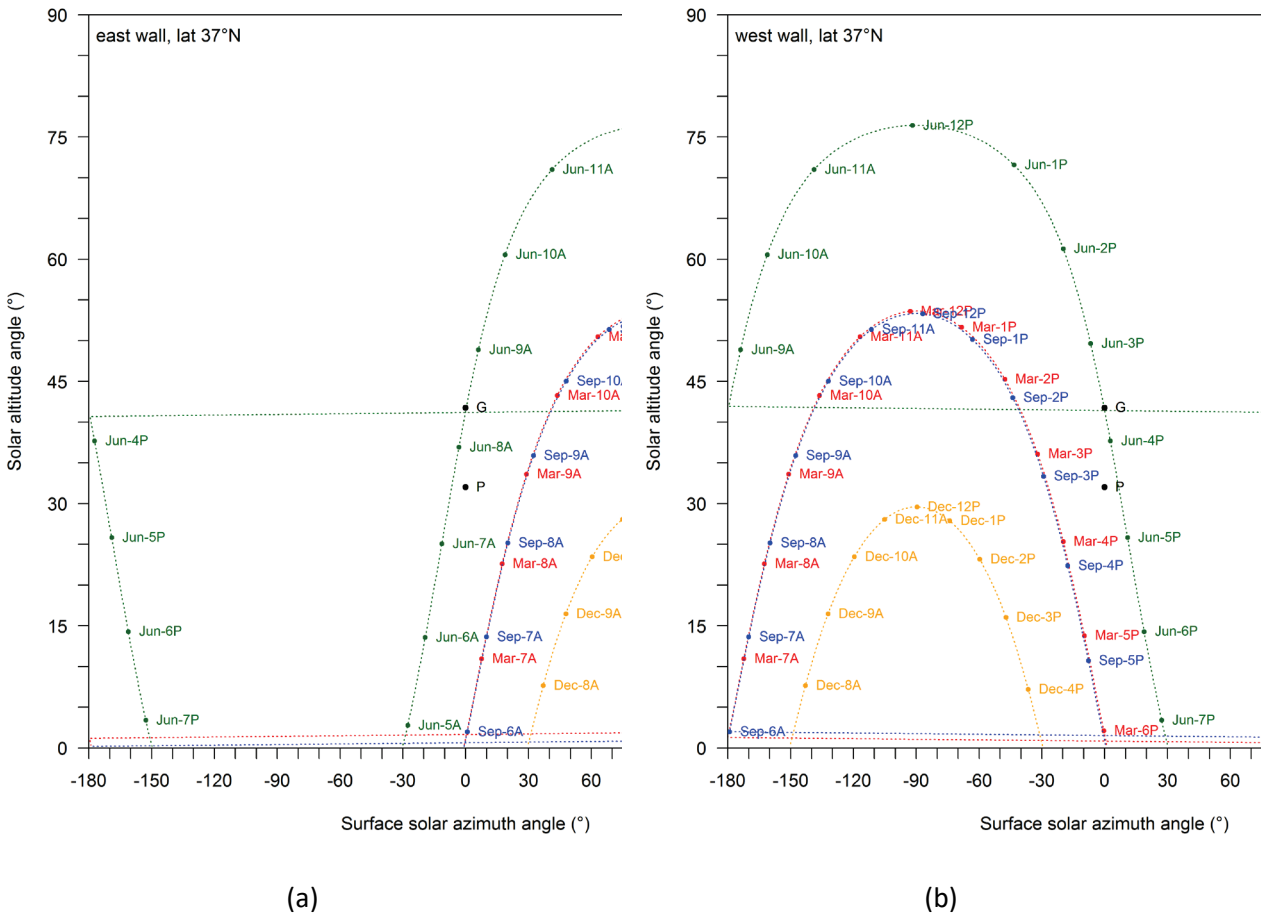

Figure 14. Solar trajectories (position versus local standard time) on Mar 21 (vernal equinox), Jun 21 (summer solstice), Sep 21 (autumnal equinox), and Dec 21 (winter solstice) across (a) east, (b) west, (c) south, and (d) north walls at latitude 37°N. Note that surface solar azimuth angle = solar azimuth angle – surface azimuth angle.

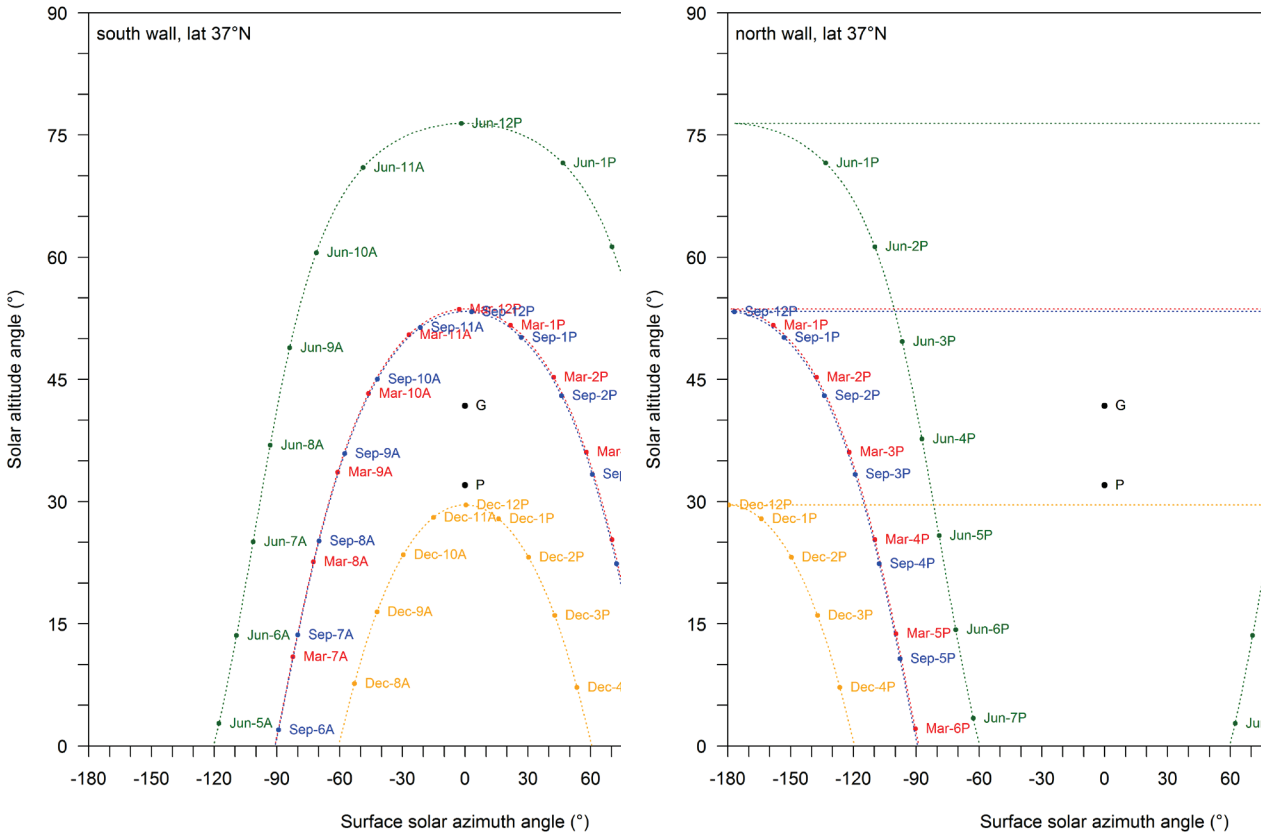

(c) (d)

Figure 14 (continued)

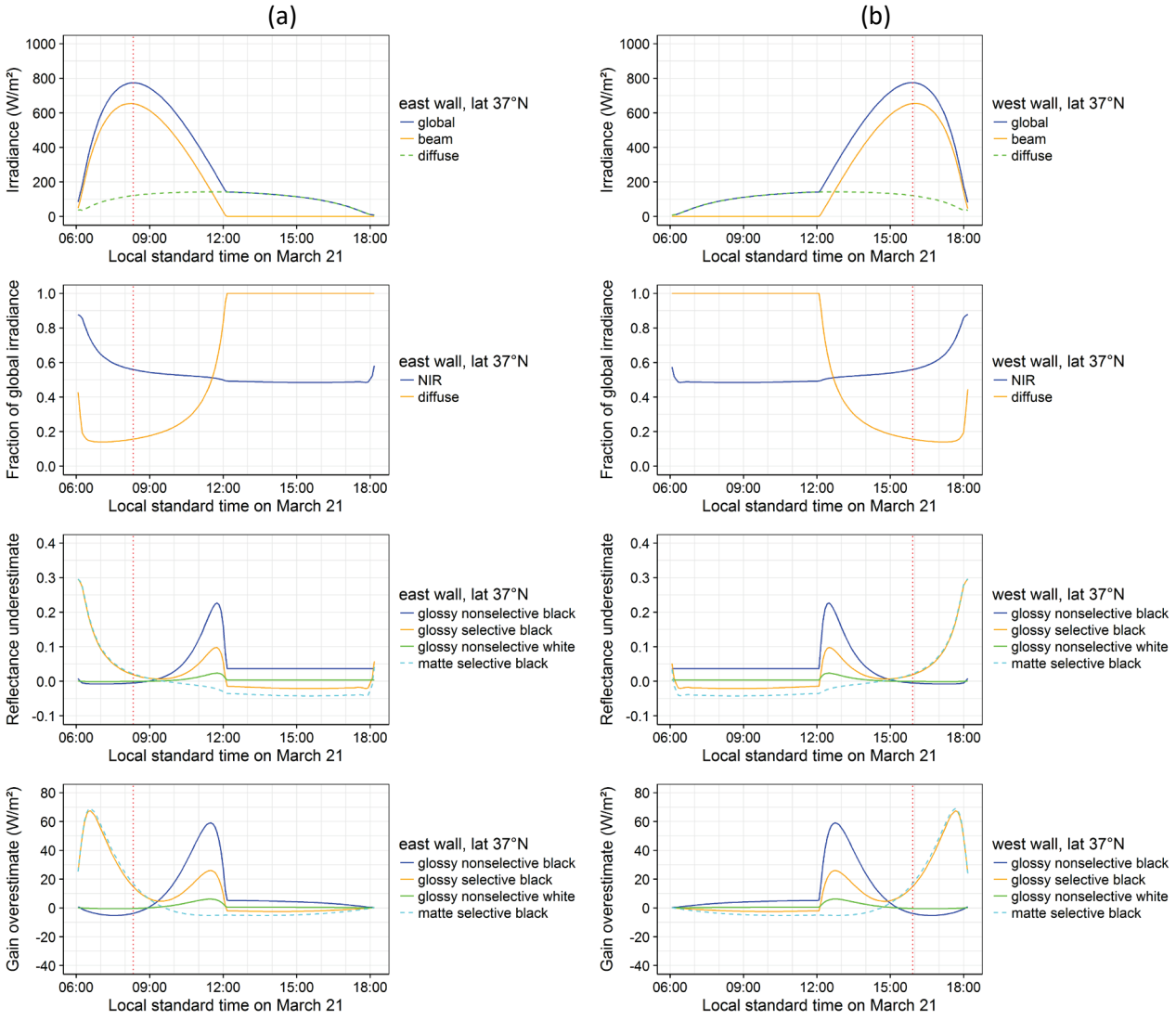

Figure 15. Top to bottom: time series on Mar 21 of global, beam, and diffuse tilt solar irradiances; NIR and diffuse fractions of global solar irradiance; underestimation of global solar reflectance, $R_g(t) – R^*$; and overestimation of solar heat gain, $I_g(t)$ [$R^* - R_g(t)$], shown for (a) east, (b) west, (c) south, and (d) north walls at latitude 37°N. Dotted red vertical line marks time of peak global solar irradiance.

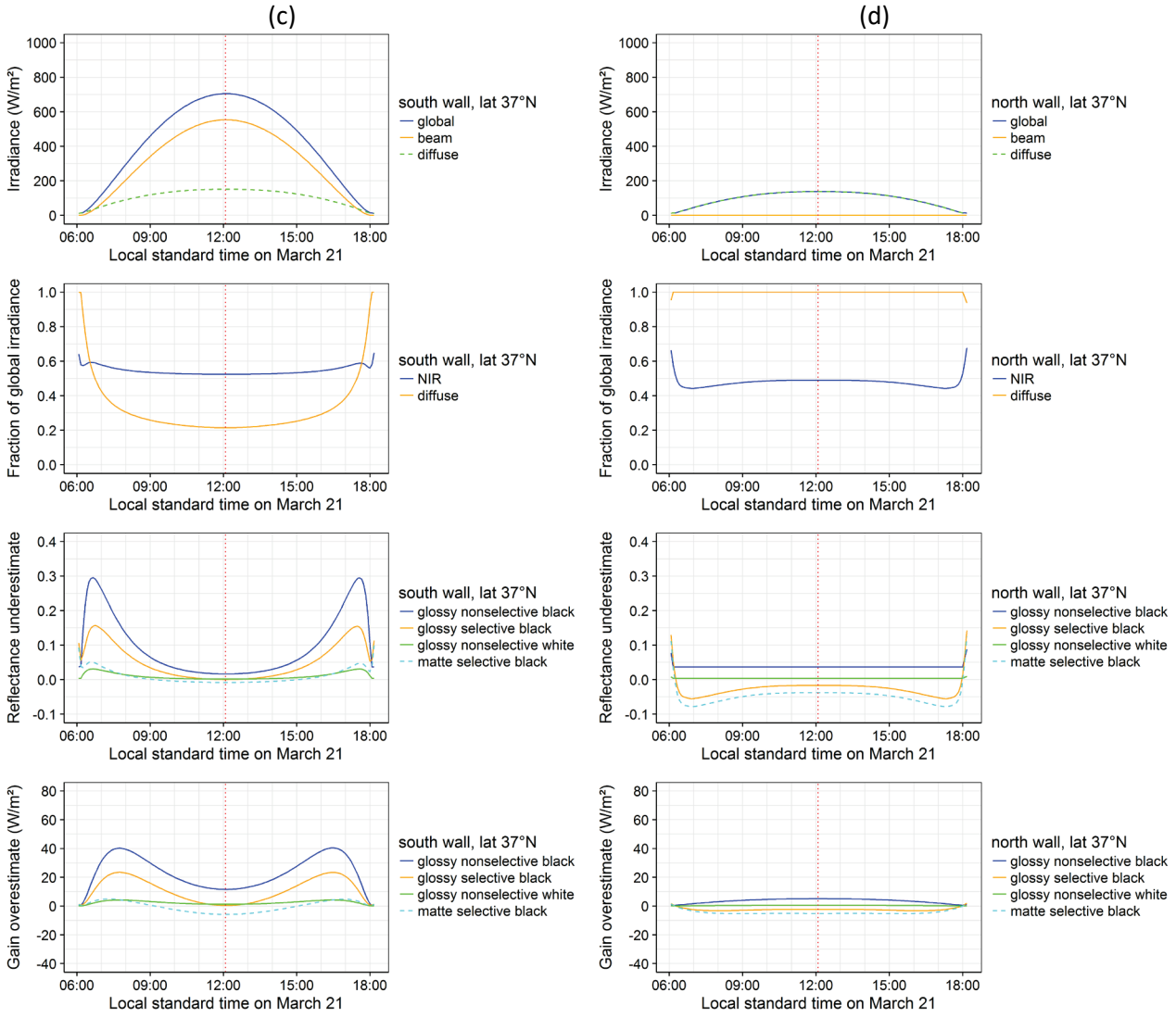

Figure 15 (continued)

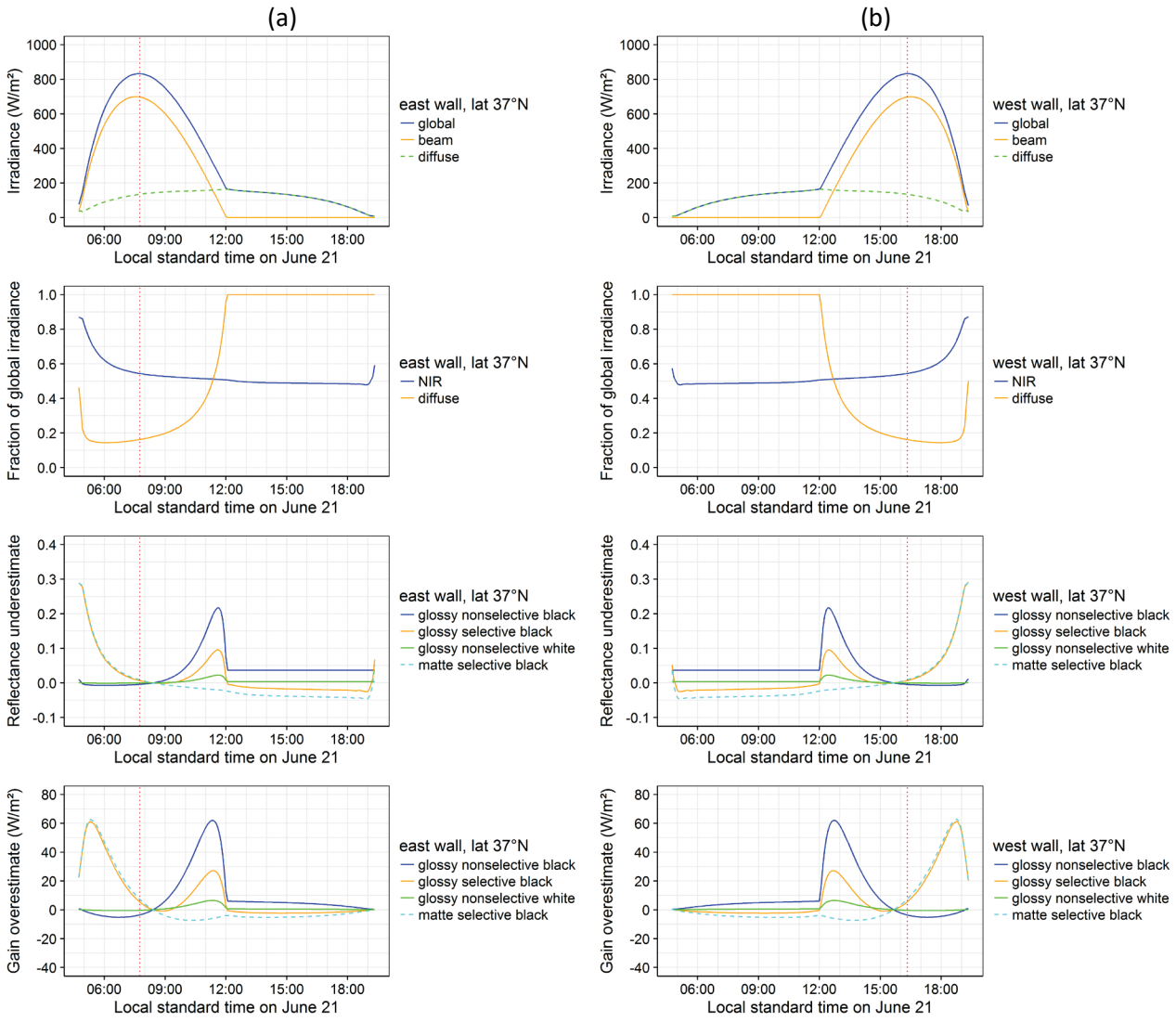

Figure 16. Time series from Figure 15 evaluated on June 21.

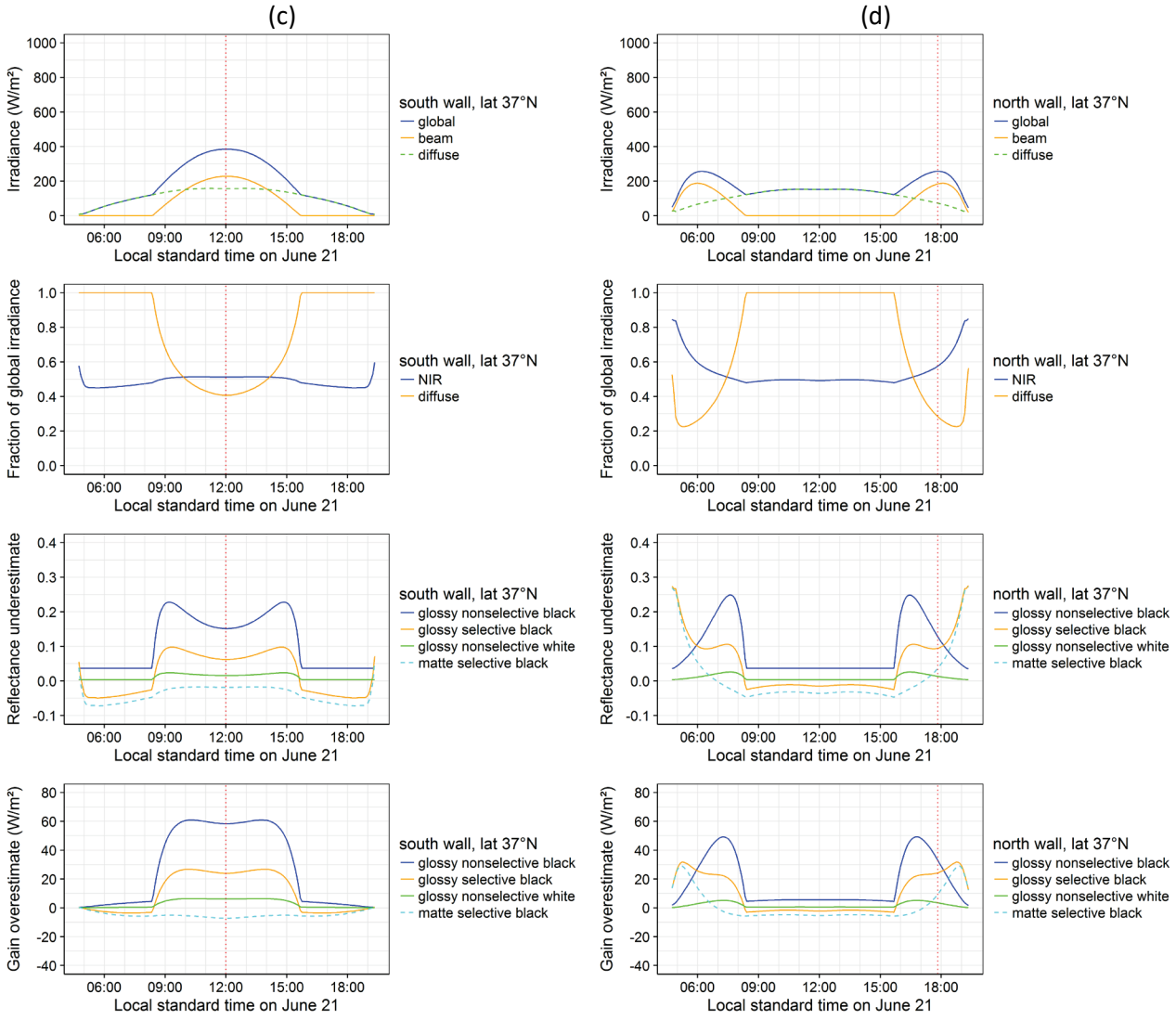

Figure 16 (continued)

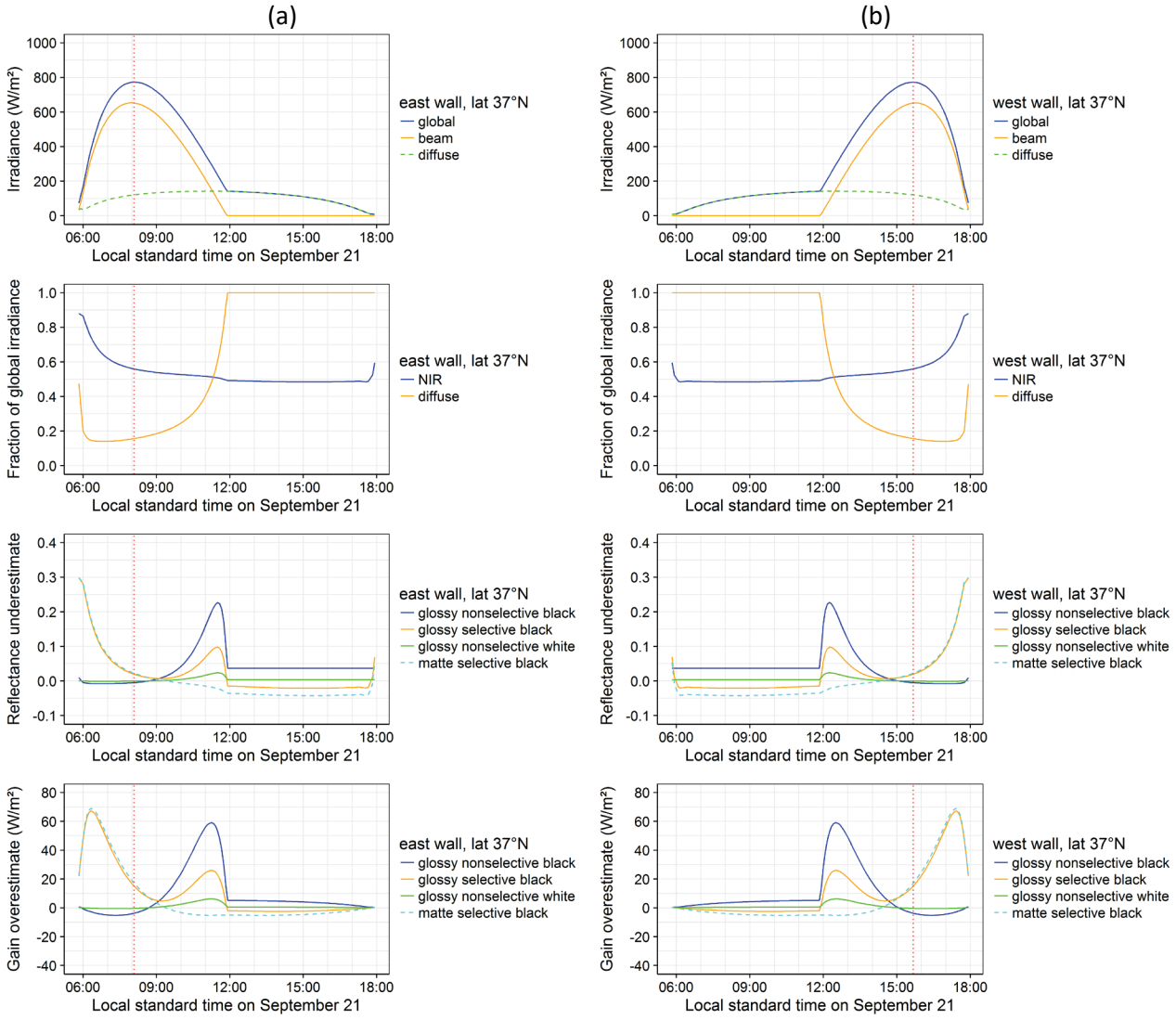

Figure 17. Time series from Figure 15 evaluated on September 21.

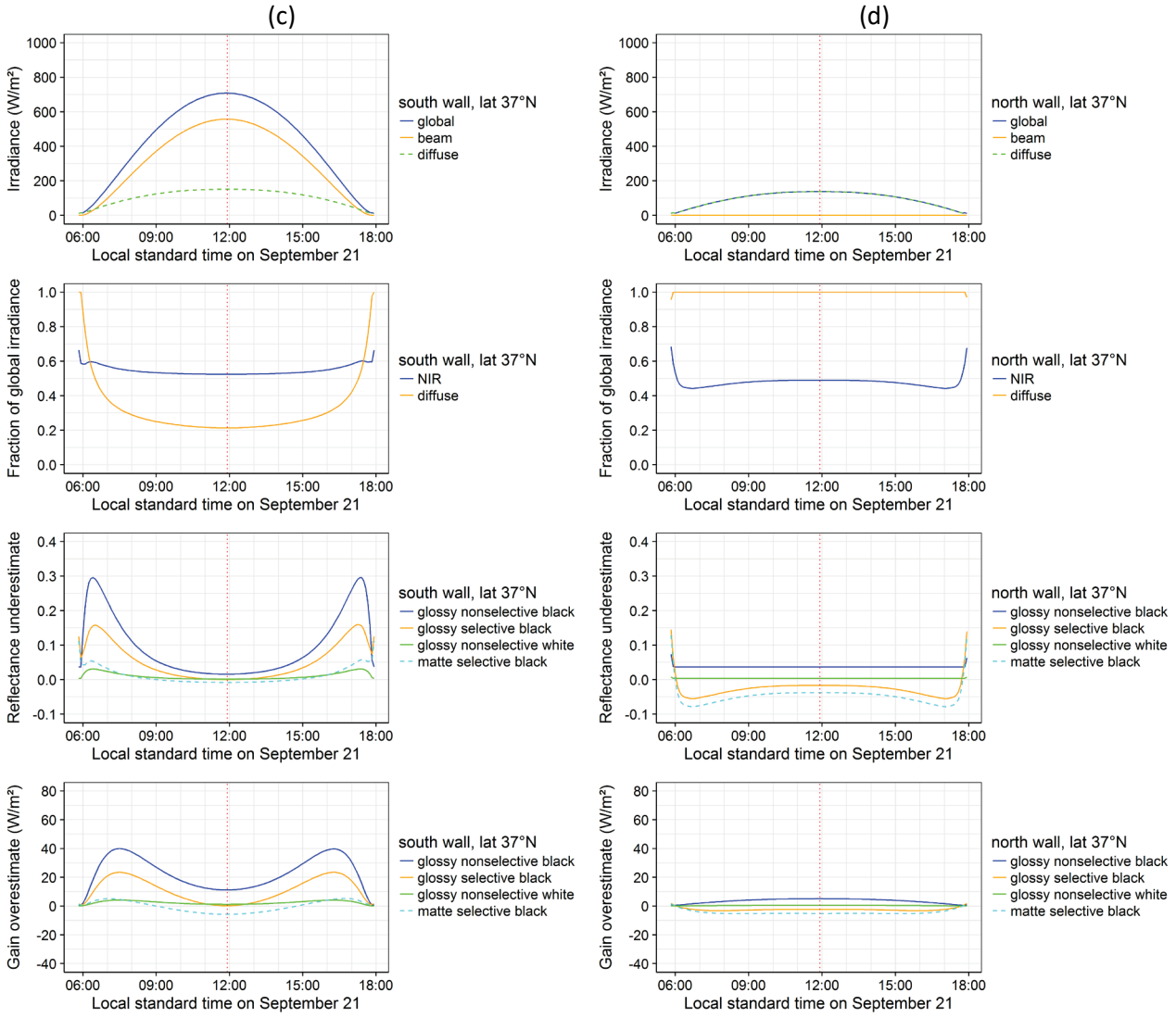

Figure 17 (continued)

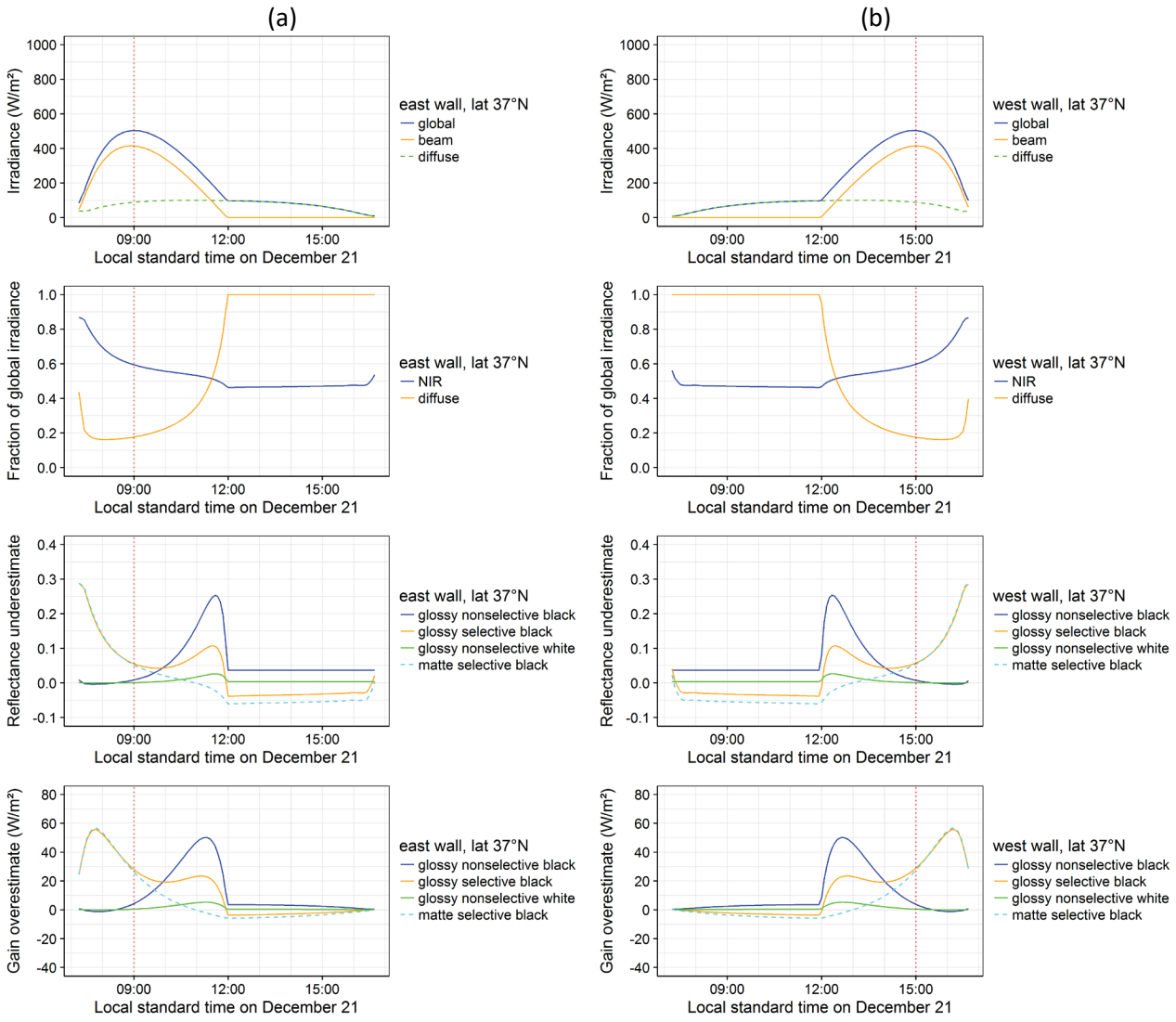

Figure 18. Time series from Figure 15 evaluated on December 21.

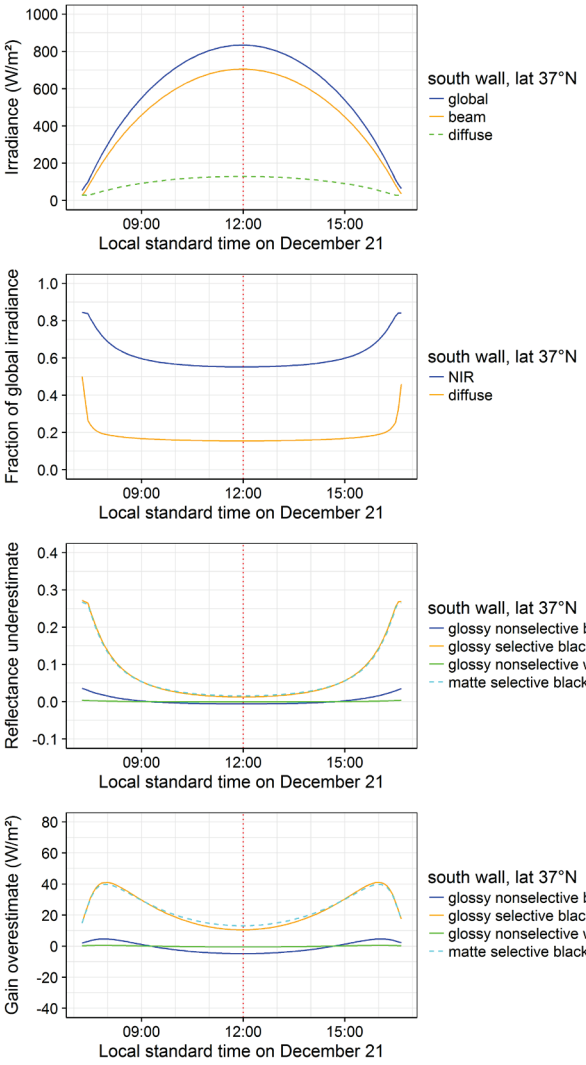

(c)

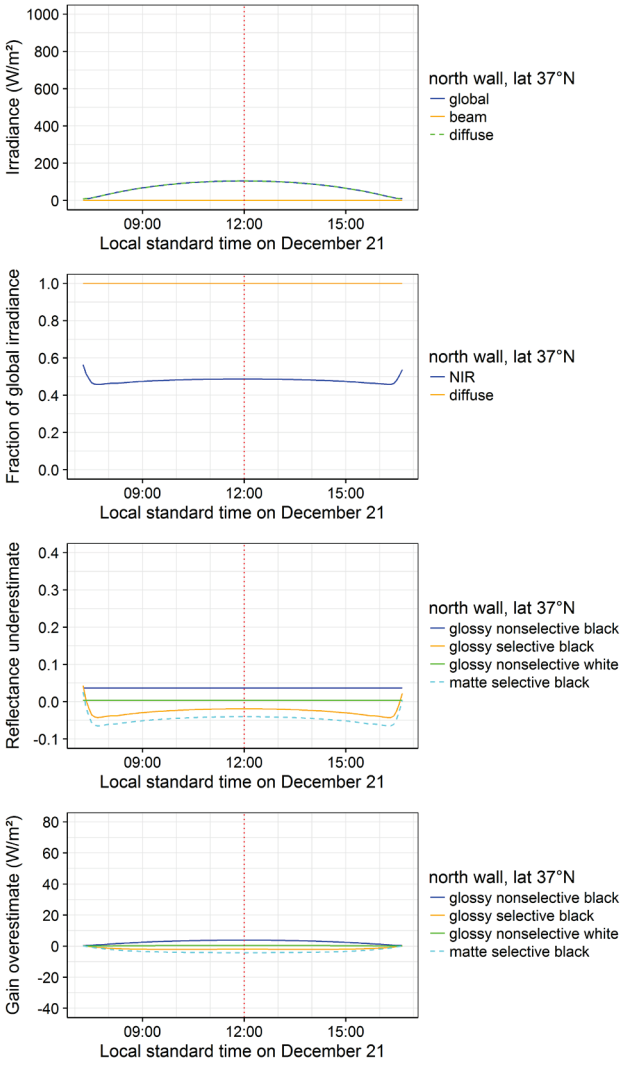

(d)

Figure 18 (continued)